Contents lists available at ScienceDirect

Saudi Journal of Biological Sciences

journal homepage: www.sciencedirect.com

Original article

Poloxamer-chitosan-based Naringenin nanoformulation used in brain targeting for the treatment of cerebral ischemia

Niyaz Ahmad [a,b,*], Rizwan Ahmad [c], Farhan Jalees Ahmad [d], Wasim Ahmad [e], Md Aftab Alam [f], Mohd Amir [c], Abuzer Ali [g]

[a] Department of Pharmaceutics, College of Clinical Pharmacy, Imam Abdulrahman Bin Faisal University, Dammam, Saudi Arabia
[b] Department of Pharmaceutical Chemistry, College of Clinical Pharmacy, Imam Abdulrahman Bin Faisal University, Dammam, Saudi Arabia
[c] Department of Natural Products and Alternative Medicine, College of Clinical Pharmacy, Imam Abdulrahman Bin Faisal University, Dammam, Saudi Arabia
[d] Nanomedicine Lab, Department of Pharmaceutics, School of Pharmaceutical Education and Research, Jamia Hamdard, Hamdard Nagar, New Delhi, India
[e] Department of Pharmacy, Mohammad Al-Mana College for Medical Sciences, Safaa, Dammam-34222, Saudi Arabia
[f] Department of Pharmaceutics, School of Medical and Allied Sciences, Galgotias University, Gautam Budh Nagar, Greater Noida 201310, India
[g] College of Pharmacy, Taif University, Taif 21974, Saudi Arabia

ARTICLE INFO

ABSTRACT

Objective: Here, the aim is to improve the bioavailability of Naringenin (NRG) in brain and to establish the highest remedial benefit from a novel anti-ischemic medicine i.e. NRG.

Methods: A novel Naringenin-loaded-nanoemulsion (NE)-(*in situ*)-gel (i.e. thermoresponsive), was formulated with the help of Poloxamer-407 (20.0% w/v). Chitosan (CS, 0.50% w/v) was used to introduce the mucoadhesive property of NE-(*in situ*)-gel and finally called as NRG-NE-gel + 0.50%CS. A novel UHPLC-ESI-Q-TOF-MS/MS-method was optimized and used for NRG-NE-gel + 0.50%CS to quantify the Pharmacokinetic-(PK)-parameters in plasma as well as brain and to evaluate the cerebral ischemic parameters after MCAO i.e. locomotor activity, grip strength, antioxidant activity, and quantity the infarction volume in neurons with the safety/toxicity of NRG-NE-gel + 0.50%CS after i.n. administration in the rats.

Results: The mucoadhesive potency and gelling temperature of NRG-NE-gel + 0.50%CS were observed 6245.38 dynes/cm^2 and 28.3 ± 1.0 °C, respectively. Poloxamer-407 based free micelles size was observed 98.31 ± 1.17 nm with PDI (0.386 ± 0.021). The pH and viscosity of NRG-NE-gel + 0.50%CS were found to be 6.0 ± 0.20 and 2447 ± 24cp (at 35.0 ± 1.0 °C temperature), respectively. An elution time and m/z NRG were observed 1.78 min and 270.97/150.96 with 1.22 min and m/z of 301.01/150.98 for Quercetin (IS) respectively. Inter and intra %precision and %accuracy was validated 1.01–3.37% and 95.10–99.30% with a linear dynamic range (1.00 to 2000.00 ng/ml). AUC_{0-24} of plasma & brain were observed 995.60 ± 24.59 and 5600.99 ± 144.92 (ng min/ml g) in the rats after the intranasal (i.n.) administration of NRG-NE-gel + 0.50%CS. No toxicological response were not found in terms of mortalities, any-change morphologically i.e. in the microstructure of brain as well as nasal mucosa tissues, and also not found any visual signs in terms of inflammatory or necrosis.

Production and hosting by Elsevier

Conclusion: Intranasally administered NRG-NE-gel + 0.50%CS enhanced the bioavailability of Naringenin in the brain. In the cerebral ischemic rats, significantly improved the neurobehavioral activity (locomotor & grip strength) followed by antioxidant activity as well as infarction volume. Finally, the toxicity studies carried out and established the safe nature of optimized-NRG-NE-gel + 0.50%CS.

1. Introduction

Brain ischemia is the 2nd largest neurological disease because of it's causes the disability together with morbidity and mortality. Ischemic brain caused the permanent worsening of CNS due to this reason, constructed the stroke (Ahmad et al., 2019a; Ahmad et al., 2018a; Ahmad et al., 2018b). On the basis or previously published data, oxidative stress was the major contributor of the cerebral ischemia development and their reperfusion injury. Largest quantity of oxygen consumption due to the production of free radicals and reactive oxygen species (ROS) at the time of oxidative stress in the body (Ahmad et al., 2018c; Ahmad et al., 2013; Ahmad et al., 2017a). Inflammatory cells released the free radicals due to defense mechanism is not properly worked by brain that affects the tissue viability in the surrounding areas. Therefore, it acts as a source of pathogenesis for ischemic-reperfusion injury (Ahmad et al., 2013; Raza et al., 2013).

Naringenin (NRG, 5,7,4-trihydroxyflavanone) is a naturally acting flavonoid compound present in the tomatoes and grapefruits. NRG has been confirmed so many therapeutic applications with anti-inflammatory action (Raso et al., 2001), anti-oxidative effect (Renugadevi et al., 2009), and also proved that Naringenin is used in the treatment of cerebral ischemia (Raza et al., 2013; Bai et al., 2014; Wang et al., 2017a). NRG has a great scavenging property for oxygen-free radicals and also chelating the metals. NRG also contains a property to inhibit the enzymes to thwart oxidation of LDL (i.e. Low-Density Lipoproteins). The most important draw back with Naringenin exhibited a very poor bioavailability and insolubility of the water (Madsen et al., 2000; Yu et al., 2005). We have design a innovative lipid-based-drug-delivery-systems for the NRG delivery to overcome these limitations and to improve the clinical therapeutic applications of NRG. We have chosen intranasal drug delivery to improve bioavailability (BA) of NRG along with reducing toxicity and their dose. It will be a great help to solve this problems related with NRG in terms of BA, toxicity, and dose reduction. Furthermore, the intranasal route has another most important application to avoid the extra time for the binding of more plasma protein and made them availability of more quantity of drug freely to give us higher therapeutic effect. NRG exhibited low molecular weight drug i.e. 272.257 g/mol with high partition coefficient; it is very beneficial to design the NRG-loaded-nanoformulation that will be easily permeated via olfactory epithelial membrane. NRG has been selected now for CNS targeting will be loaded in a newly develop and optimize nanoformulation via intranasal administration.

Though, the most important challenge for the nanoformulation/drug carrier will maintain the required time in the nasal cavity/nasal mucosa (Zhao et al., 2016). Thermosensitive hydrogel have a great solution having the unique property to use for this obstruction. These type formulations are easily sprayed/dropped because of its low viscosity at room temperature after intranasal delivery. Most of the nasal devices are available in the markets that are designed only for solution based formulations which are easily spread extensively on the nasal cavity/nasal mucosa in the solution form. This formulated solution is converted into viscous hydrogel due to increase in the temperature (32.0 °C) in the nasal cavity/nasal mucosa when it reached to nasal cavity/nasal mucosa. After that it will decrease the mucociliary clearance rate from the nasal cavity/nasal mucosa and drug releases in sustained release form (Liu et al., 2016). The most important application of this type of system has showed their strength to absorb maximum amount of biological fluids or water (Agrawal et al., 2010).

Poloxamer are commonly used for thermosensitive hydrogel forming agent particularly Poloxamer-407 (Cabana et al., 1997). Poloxamer-407 was used previously for NRG-loaded-nanosuspension/nanostructured lipid carriers as a drug delivery system (Raeisi et al., 2019; Sumathi et al., 2017). We will prepare a nanoemulsion in which Naringenin (NRG) will be encapsulated into a nanoemulsion. After that, optimized nanoemulsion will convert again into an *in situ* gel with the use of Poloxamer-407. Poloxamer-407 will be used because it's already reported their safe nature and to use as a *in situ* gelling agent of formulations for the intranasal as well as ocular delivery of many drugs (Gratieri et al., 2010; Fakhari et al., 2017; Salatin et al., 2017). Poloxamer-407 is a tri-block copolymer containing 1-monomor which is made up of one polypropylene oxide chain and 2-polyethylene oxides. Structurally, hydrophobic core is made up of 1-polypropylene oxide chain and 2-polyethylene oxides constructed hydrophilic corona. These 3-blocks of Poloxamer-407 form polymeric nanomicelles when it goes to self-orientation in the aqueous media with greater CMC (0.35%) level (Rey-Rico et al., 2015). At the 2.0 to 15.0 °C temperature, polyethylene oxides is soluble; the micelles formation takes place > 15.0 °C temperature and then formation of gel due to dehydration reaction (Bonacucina et al., 2008). *In situ* gel formulated from Poloxamer-407 that contains so many advantages like steric stability of NE, unaffected by nasal aerodynamics and mucociliary clearance. In addition it represents optimum mucoadhesive potency (w/v: 0.50%; chitosan concentration: 0.50% CS) and finally, it was formulated as NRG-NE-Gel + 0.50%CS.

The major objective of proposed current research was to achieve i.n. drug-delivery to the brain with improve retention time followed by mucoadhesive properties in the treatment of cerebral ischemia. *In situ* gel was formed by the use of CS and poloxamer; it was used as a gelling agent previously and later on used as a mucoadhesive agent in the current study. The most important one more objective of current research was to compare NRG-S (NRG-suspension) with NRG-NE-Gel + 0.50%CS for the calculation of pharmacokinetic parameters (brain bioavailability, NRG-NE-Gel + 0.5%CS intranasal application, and i.v. with i.n. administration of NRG-NE-Gel + 0.50%CS & NRG-S). We required an easy, less time consuming, sensitive, robust, as well as highly reproducible bioanalytical method for the quantification NRG in the brain and blood samples as per the evaluation of pharmacokinetic parameters. There are so many analytical methods are reported for the quantification of NRG but not a single bioanalytical method reported for brain or brain homogenate samples for the brain-PK including for the quantification of NRG as single analyte with high robust method (Sun et al., 2014; Wang et al., 2014; Magiera et al., 2012; Baranowska et al., 2016a; Baranowska et al., 2016b). The most important parameter for the estimation of NRG-bioanalytical

method (upto nanogram i.e. ng/mL in the brain as well as plasma samples) has not been reported till date that should be reproducible and roughest.

This is a first time research; a novel-nano-formulation (NRG-NE-Gel + 0.50%CS) will be formulated and apply through intranasal route. A novel bioanalytical method will be developed and validated which will be highly sensitive, easy, and rapid for the estimation of NRG brain-homogenate as well as plasma samples by the highly sensitive instrument i.e. UHPLC-ESI-Q-TOF-MS/MS.

2. Experimental

2.1. Materials and methods

NRG, Chitosan (75.0 to 85.0% degree of deacetylation) (Sigma-Aldrich, St Louis, MO, USA), Poloxamer 407, 2,3,5-Triphenyltetrazolium chloride (TTC) and EDTA (Sigma-Aldrich Chemicals Pvt. Ltd., India) were bought. Tween-80, PEG-400, and remaining surfactants were bought from Sigma Life Science, Sigma Aldrich (Belgium). Methanol and Acetonitrile (HPLC-grade) were bought from SD-Fine Chemicals, Ltd whereas deionized water was purified with the help of Milli-Q water purification system (Millipore, Bedford, MA, USA).

2.1.1. Preparation of Naringenin nanoemulsion (NRG-NE)
Naringenin as a drug (2.0% w/v), Capmul MCM (2.0% v/v oil), and Tween-80 and PEG-400 (4:1) as a Smix (10.0% v/v) were used for the preparation of NRG-NE. A little quantity of NRG was dissolved in Capmul MCM as an oil phase and rest of them were dissolved in Smix. A 10.0 ml borosilicate glass vial was used 200 μL NRG in the oil. For the preparation of oil-surfactant mixture, 1.0 Smix was added into the same vial. Ultra high pure-water (6.40 ml) was titrated the oil-Smix mixture (1.30 ml). Finally, we prepared the NRG–NE (7.70 ml). At the end, we added CS-Solution (i.e. 2.3 ml). Ultrasonication (Fisher Scientific Technology, USA) were used to reduce the globule size of prepared NRG-NE for the 1.0 min (Ahmad et al., 2019b)

2.1.2. Preparation of thermosensitive in situ gel
We have prepared firstly the chitosan solution (2.0%w/v, CS) for the conversion of NRG–NE into a thermosensitive-mucoadhesive *in situ* gel. In a brief, CS (200.0 mg) was solubilized into glacial acetic acid (1.0% v/v, 10 ml). 2.30 ml CS (2.00%w/v) was added to mixed it properly with NRG–NE (7.70 ml) for the conversion of NRG–NE into a thermosensitive-mucoadhesive *in situ* gel. 20.0% w/v Poloxamer-407 (2.0 g) was added to this last prepared mixture followed by continuous stirring. Temperature (<4.0 °C) was maintained by crushed ice at this time processing. NRG–NE–gel + 0.50%-chitosan (final nanoformulation) was stored in the refrigerator (<4.0 °C) for 18.0 h. But time to time, NRG–NE–gel + 0.50%chitosan stirred to solubilized the Poloxamer–407 entirely (Barakat et al., 2017; Mendonça et al., 2016; Ahmed et al., 2019).

2.1.3. Characterization of thermosensitive in situ gel
2.1.3.1. Temperature at the time of gelation.
Temperature at the time of Gelation or gelling point is the most important point that is a maintenance point for a thermoresponsive-*in situ*-gel. Xu et al. (2014) reported a method for gelling point determination; we have followed same method for the determination of gelling point but done small changes. In brief, 10.0 ml of NRG-NE-gel + 0.50%CS solution was transferred into the borosilicate vial and kept under the hot-plate-digital-magnetic-stirrer. Hot-plate temperature was slowly-slowly increased with a 1.0 °C/min rate. At this time, magnetic bead was revolved at 100 rpm speed. Revolution of magnetic-bead was stopped when NRG–NE–gel + 0.50%CS-gelling-point was observed visually. At this point, the temperature was noted as a gelation temperature through the dipped digital thermometer (Xu et al., 2014; Ahmed et al., 2019c).

2.1.3.2. Hydrodynamic diameter, polydispersity index (PDI), zeta potential and SEM.
Dilution of NRG–NE–gel + 0.50%CS was performed upto 100.0 times and after that sonicated with the help of bath-sonicator till all the small bubbles cleared at the time of analysis of PDI and globule size. PDI and globule size of *in situ* gel were examined through Malvern Zetasizer i.e. based on dynamic light scattering technique at a scattering angle of 90°. At the time of this entire analysis temperature was maintained at 25.0 ± 1.0 °C after that determine the zeta potential. The optimized-NRG–NE–gel + 0.50%CS samples were also evaluated by SEM (in triplicate) used by the method before Ahmad et al. (2019c).

2.1.3.3. SEM and TEM study.
Texture of NRG-NE-gel + 0.5%CS surface was assessed by the SEM procedure (Zeiss EVO40; Carl Zeiss; Cambridge; UK). The NRG-NE-gel + 0.50%CS-sample was spread and adhered by the SCD-020-Blazers-sputter-coater-unit with the help of use of Ar-gas (50.0 mA for 100.0 s), a pre-maintenance-unit was confirmed (Ahmad et al., 2019c). TEM (Morgagni 268D; FEI Company, Hillsboro, OR) was used for the NRG-NE-gel + 0.50% CS samples were formulated on the Cu-grid after the dilution (50.0 times) of the gel. Phosphotungstic acid (2.0%) was used as a contrasting agent at the time of sample preparation and imaging under high vacuum selection mode (Ahmad et al., 2019c).

2.1.3.4. Mucoadhesion evaluation (ex vivo) of nanoformulation based on Curcumin (Cur) by confocal laser scanning microscopy (CLSM).
Curcumin (Cur) is a food coloring agent with yellow color and contains same fluorescent properties to the fluorescence-Na. At the 550.0 nm spectral-region, Cur showed strong-fluorescence at 488.0 nm due to excitation. At 590.0 nm, the fluorescence signal was identified which contains a distance for the background fluorescence (Otberg et al., 2004). Cur-dye is soluble in oil, therefore we added at the time of formulating the NE. All the samples were analysed in three different samples. For the determination of retention time of nasal mucosa of Cur-(NRG-NE-gel + 0.50%CS), we were washed nasal mucosa three-time on the every five-minutes gap with normal saline as a specimen. All the specimen samples were mounted as it is on the glass slide i.e. upside position is mucosal side position. Now, we have determined the samples through CLSM (Olympus-Fluo-View-FV-1000, Hamburg, Germany). Green helium neon laser beam were measured at 543.0 nm for the all mounted nasal mucosa samples. 20X was set to examine the all images. Cur-(NRG-NE-gel + 0.50%CS) penetration was confirmed and captured by the serial 4.4 m optical sections with the Z-axis (Otberg et al., 2004).

2.1.3.5. Determination of pH and their viscosity.
NRG-NE-gel + 0.50% CS-pH was calculated through pH meter (Eutech pH Tutor, Effem Technologies, India) were properly calibrated before. NRG-NE-gel + 0.50%CS viscosity were determined by the cup and bob type of Brookfield viscometer (DV II + Pro, U.S). The gel having cup was kept in a water bath and the temperature was fixed 35.0 ± 1.0 °C. Rate of shear was applied 60 rpm on the NRG-NE-gel + 0.50%CS by the spindle no. 64 (Singh et al., 2013).

2.1.3.6. In vitro gel erosion study.
NRG-NE-gel + 0.50%CS erosion time study was carry out to evaluate the time for NRG-NE-gel + 0.50%CS degraded or dissolved entirely due to the body fluid effect. There are donor and a receptor part in the franz-diffusion cell. In between the donor and receptor compartment were kept the dialysis membrane (MWCO~12–14 kD). Thermosensitive-

NRG-NE-gel + 0.50%CS (i.e. 110.50 mg) was kept on the dialysis membrane. The weight was taken for the entire setup except receiver medium. Phosphate-buffer (pH: 6.40) was kept in the receiver section and maintained the whole assembly at 37.0 ± 1.0 °C with 100.0 rpm. NRG-NE-gel + 0.50%CS was evaluated on the basis of visual observation and determined the quantity at every selected-time intervals until the entire NRG-NE-gel + 0.50%CS were dissolved. At every time interval, the whole release medium was taken out and dried the receptor compartment once more time; the complete apparatus was weighed again. Once more time receiver medium was kept freshly in the receptor side.

At a specific time interval calculation, Eroded quantity of NRG-NE-gel + 0.50%CS = initial weight of the setup – Final weight of setup. Receiver medium was included at time of calculations. The graph was drawn in-between percentage of NRG-eroded (on the Y-axis) vs. time (on the X-Axis in min) (Zhang et al., 2002).

2.1.3.7. NRG-permeation study (ex-vivo). Ex vivo permeation study was performed on the diffusion cell system (LOGAN SFDC-6; Logan Instruments Corporation, USA). 3-separate-franz diffusion cells were associated with thermostat.

Every-franz diffusion cells exhibited the 1.0 ml cell cap and 5.0 ml cell body in which the defined permeation area (0.60 cm^2) is fixed. Nasal mucosa were removed and freshly used. It was mounted in-between cell caps and cell bodies whereas the mucosal side faces upper side. Before going to start nasal permeation study, phosphate buffer saline (PBS, 5.0 ml, pH: 6.40) and ethanol [70:30 v/v ratio] were taken for all types of formulations. The most important thing is equilibration of nasal mucosae with PBS at 35.0 ± 1.0 °C and 100.0 rpm for 15.0 min. NRG-NE-gel + 0.5%CS, NRG-NE, NRG-S (1.0 ml) were kept into their respective cell chambers. The samples (1.0 ml) were collected on already selected time points (0.500, 1.00, 2.00, 3.00, 4.00, 6.00, 8.00, and 12.00 h) for the calculations of NRG-permeation through UHPLC-MS/MS method (mentioned in this manuscript). The samples were taken precise quantity from the cell bodies and after that same amount of media transferred freshly (Ahmad et al., 2018d). A graph was drawn in-between percentage of cumulative NRG-permeated (on the Y-axis) vs. time (on the X-Axis in min) for the comparison of all 3-formulations permeation study. This permeation graph helps in the calculation of flux (μg/cm^2/h) which is total quantity of NRG-permeated/cm^2 (TQNP/cm^2) at Y-axis and on X-axis (time: hours). For the kinetic study model, Korsmeyer-Peppas, Higuchi, first order, zero order equations were checked with permeation-NRG data, all these equations were fitted with our permeation-NRG data (Ahmad et al., 2018d; Ahmad et al., 2017b).

2.2. In vivo study

2.2.1. Experimental study on animals

The authors have taken the approval from Jamia Hamdard ethical committee, India which follows the national guidelines used and care of laboratory animals. This approval is based on the study included the parameters like PK, histopathological, biodistribution, biochemical estimation, and neurobehavioral studies in wistar rats. When we are going to start the experiment, all the rats (8 to 10 weeks old, 300.0 to 400.0 g) were issued from central animal house. We maintained the environmental conditions like humidity 60.0 ± 5.0%, temperature 25.0 ± 2.0 °C, and 12.0-h dark–light cycle whereas a high quality fed with reference-pellet-diet.

2.2.2. UHPLC/ESI-Q-TOF-MS/MS based bioanalytical method development and their validation

We have used the Waters-ACQUITY UHPLC^{TM} system (Waters Corp., MA) for the bioanalysis with tunable MS/MS detector from (SYNAPT; Waters Corp., Manchester, UK). For chromatographic separation, we have used the column (1.7 μm; 2.1 × 100 mm). Mobile phase was consisted of acetonitrile (90.0%):2mM ammonium acetate (10.0%): formic acid (0.01%) [v/v/v] at a 0.25 ml/min flow rate with 10.0 μL injection volume for Q-TOF-SYNAPT Mass were used as operated in V-mode followed by the resolution 32000.0 mass and 1.0 min scan time with the 0.020 s inter-scan time as well as 5.3 × 10^{-5} Torr pressure for collision gas used. Trap collision energy (Trap-CE) were used as 19.39 eV and 21.46 eV to get the transitions at *m/z* 270.9/150.9, 301.0/150.9 for NRG and IS (Quercetin), respectively. The concentrations have taken 8-non-zero concentrations (1.0; 2.0; 31.0; 420.0; 850.0; 1300.0; 1700.0; & 2000.0 ng/ml) and 2.0% spiked aqueous standards in the blank lungs-homogenate, plasma, and brain homogenate samples, it means 20.0 ml aqueous sample + 980.0 ml blank matrix samples. 3-different concentrations of samples for quality control (QC) i.e. 1600.00 ng/mL for higher-level-QC (1600.00 ng mL^{-1} HQC), medium-level-QC (810.0 ng mL^{-1} MQC), followed by the lower-level-QC (3.0 ng mL^{-1} LQC) were prepared. All CC and QC-matrix spiked-samples were stored in the deep freezer at a temperature –80.0 °C. For the matrix extraction of samples, all CC and QC samples were taken 550.0 μL along-with 100.0 ng mL^{-1} IS (50.0 μL), and added 150.0 μL, 5.0% formic acid-solution in each and individual test tube for every CC and QC sampling time point followed by mixed and vortexed properly for 5.0 min to breaking of matrix proteins for liquid–liquid extraction. Same test tube at every CC and QC sampling time point was added 5.0 ml Ethyl acetate separately with the shaking (1500.0 rpm) and then centrifugation at 4.0 °C for 10.0 min at 4000.0 rpm. At last, 4.0 ml supernatant sample solution were transferred into a new test tube for drying N$_2$-evaporator and then reconstituted again with the mobile phase (550 μL) with the help of vortexer followed by transferred into UHPLC-vials for bioanalysis. For NRG-bioanalytical method development and their validation, we were used US-FDA, 2018 guidelines. For the concentration-detector response-ratio, we have used regression-equation with 1/x^2-factor response curve [NRG (Drug) to QUR (IS) concentration-ratio. All the validation parameters were validated on the basis of US-FDA, 2018 guidelines adopted by (Ahmad et al., 2018a; Ahmad et al., 2018d; Ahmad et al., 2017b).

For the calculation of stability (%), below formula was utilized:

$$\text{Stability } (\%) = \frac{\text{Mean observed response of stability QCs}}{\text{Mean theoretical} - \text{response of comparison QCs}} \times 100$$

2.2.3. Biodistribution, pharmacokinetics, brain drug-targeting potential with brain-targeting efficiency

4-groups of wistar-rats (male) with 3-individual wistar-rats (male) at every sampling point (Total sampling point = 7) (Total rats = 84 [(7 × 3) = 21 × 4 = 84] were taken for the analysis of study PK & biodistribution study. In brief; NRG-Suspension, & NRG-NE-gel + 0.5%CS (body weight of 10.0 mg kg^{-1} equivalent dose) were given individually through i.v. as well as i.n. route after that the collected the blood samples at pre-selected time-points (0.50, 1.0, 2.0, 4.0, 8.0, 12.0 and 24.0 h) followed by the pre-treatment and extracted the collected different matrix-samples as well as analysed as per the US-FDA, 2018 guidelines through UHPLC/ESI-Q-TOF-MS/MS". All the determined data for matrixes were calculated as C$_{max}$, t$_{1/2}$ and AUC $_{(0-t)}$. 84-wistar rats were taken to perform the biodistribution study for all selected 4-groups mentioned above.

At each and every time intervals were sacrificed 3-rats to determine the LH, plasma, and BH concentration as per the bioanalysis data obtained mentioned in the Bioanalytical method development and validation by UHPLC/ ESI-Q-TOF-MS/MS. Obtained data were

utilized to evaluate the NRG-targeting efficiency for brain (%DTE) and NRG-targeting potential for brain (%DTP) with the applied formulae (Ahmad et al., 2016a; Ahmad et al., 2018d; Ahmad et al., 2019):

$$\%DTE = (AUC_{brain} \div AUC_{blood)i.n.} / (AUC_{brain} \div AUC_{blood})_{i.v.} \times 100.0$$

$$\%DTP = (B_{in} - B_x) \div B_{in} \times 100.0$$

where $B_x = (B_{iv} \div P_{iv}) \times P_{in}$,
B_x = AUC for brain fraction (contributed by systemic circulation through BBB after i.n. administration);
B_{iv} and P_{iv}
whereas; B_{in} and P_{in} are brain and blood AUC_{0-24} after i.v. and i. n. administration, respectively.

2.2.4. Pharmacodynamic study in cerebral ischemia

6-rats were taken in each group (Total: 6-groups):
First Group: SHAM as a control group,
Second Group: SHAM + Placebo: NE-gel + 0.5%CS without NRG (as a substantial control group),
Third Group: MCAO-induced group
Fourth Group: MCAO + NRG-S (10 mg per kg body weight),
Fifth Group: MCAO + NRG-NE-gel + 0.5%CS (10 mg per kg body weight) given via i.n route.
Sixth Group: MCAO + NRG-NE-gel + 0.5%CS (10 mg per kg body weight) given via i.v. route.
Longa et al. (1989) model was used to induce MCAO via intraluminal filament. In brief; rats were anaesthetized by the chloral hydrate (i.p.; 400 mg/kg) to develop the MCAO-model in which silicone rubber-coated monofilament (4 0-3033REPK10; DOCCOL, MA) was used. In the external carotid artery have been inserted the silicone filament that continuously reached to middle cerebral artery (MCA) via internal carotid artery (ICA) to persuade MCAO. It is a confirmation through the occlusion identification in the artery. When the two hours passed, silicone filament was removed gradually. The rats were judged on the basis of neurobehavioral activity that includes grip strength and locomotor activity. When both parameters were performed the rats were scarified and removed their brains to perform the histopathological and biochemical studies.

2.2.5. Locomotor activity

Locomotor activity was performed in the digital-actophotometer as per the method adopted by Ahmad et al., 2013; Ahmad et al., 2017a; Ahmad et al., 2018b. At the time of experiment, one rat was experienced in one-time for 10 min-period duration in one-apparatus. Instruments included the square closed arena apparatus, housed in a darkened, light, infra-red sensitive photocells, and sound attenuated ventilating room.

2.2.6. Grip strength

Grip strength meter was used to determine the grip strength of rats as reported by the method Ahmad et al., 2013; Ahmad et al., 2017a; Ahmad et al., 2018b. In short; we can described simply; rat's front paws were kept on the grid and pulled down and wait for the grasping power of front's paws on the grid. When the paws were released and write it in Kg as a force/unit shown on the displayer.

2.2.7. Biochemical studies

2.2.7.1. Preparation of tissues for glutathione and antioxidant enzymes assays. After the behavioral study, the rats were sacrificed to remove the brain. This brain converted into brain homogenate (5.0%w/v) preparation, PBS (10.0 mM Phosphate-buffer, pH-7.00)

in which contains protease inhibitors (10.0 μL mL^{-1}) leupeptin (5.0 mM), 0.040% BHT (butylated hydroxytoluene), benzamidine (1.0 mM), phenylethylsulfonyl fluoride (2.0 mM), EGTA (0.10 mM), aprotinin (1.50 mM) in the centrifuge (800.0 × g at 4.0 °C for 5.0 min). For TBARS (thiobarbituric acid reactive substance) activity, supernatant (predetermined quantity, S1) were taken and then centrifuged again (10,500 X g at 4.0 °C for 15.0 min) to obtained S2 (separate post-mitochondrial supernatant: PMS) employed for evaluation of antioxidant enzymes.

2.2.7.2. TBARS (Thiobarbituric acid reactive substances). Lipid peroxidation was evaluated by the parameter of TBARS and it was used by Ohkawa et al. (1979). Briefly, BH (100 μL), thiobarbituric acid (0.670%, 1.0 ml), and trichloroacetic acid (10.0%, 1.00 ml) were taken in all the test tubes. All the test-tubes covered with Al-foil and kept in water-bath (boiling, 20.0 min). All the covered samples were kept to crush ice-bath. At last, all the samples were centrifuged at 6,000 rpm for 10.0 min. Supernatant-solution was taken into fresh test-tube for the analysis at 540.0 nm absorbance.

2.2.7.3. Glutathione reductase (GR) evaluation. Mohandas et al. (1984) was explained the method for evaluation of GR and same method followed by Ahmad et al. (2013). In a brief; a combination of different solutions (total: 2.0 ml) i.e. 0.10 mM NADPH, 0.10 M phosphate buffer with a pH 7.60, 1.0 milli-molar GSSG, and 100.0 μL PMS was used to estimate the enzyme-activity the same as calculated at room temperature when invisible of NADPH at 340.0 nm .

2.2.7.4. Glutathione peroxidase (GPx) evaluation. GPx activity was performed on the basis of Mohandas et al. (1984) method. In a brief; a combination of different solutions (total: 2.0 ml) i.e. 1.0 milli-molar EDTA, 0.10 M phosphate buffer with a pH 7.60, 1.4 U of 100.0 μL glutathione reductase, 1.0 milli-molar sodium azide, 1.0 milli-molar glutathione, 100.0μLPMS, 0.25 milli-molar H_2O_2, and 0.20 milli-molar NADPH (0.2 mM) was used to evaluate the NADPH-invisible at 340.0 nm in the room temperature. GPx activity was calculated as nM NADPH oxidized/min/mg protein by the use of molar extinction coefficient (i.e. 6.220×10^3 per mole per cm.

2.2.7.5. Catalase activity evaluation. We followed the method Ahmad et al. (2013) for the evaluation of Catalase. In a brief; a combination of different solutions (total: 3.0 ml) i.e., 0.050 M phosphate buffer with a pH 7.00, 19 milli-molar of H_2O_2, and 50.0 μL was prepared and examined the absorbance at 240.0 nm.

2.2.7.6. Super oxide dismutase (SOD). We followed the method Ahmad et al. (2013) to determine the SOD activity. In a brief; a combination of different solutions (total: 1.0 ml) i.e., 600 μL of 0.500 M PBS with a pH 7.40, 100 μL PMS (10.0% w/v), 100.0 μL of 1.00 milli-molar xanthine, and 100.0 μL of 57.0 milli-molar NBT was incubated fifteen minutes at room temperature and added the 50.0 milli-unit xanthine-oxidase successively to facilitate the start the reaction. At the 550.0 nm wavelength was measured the change in absorbance to determine the rate of reaction.

2.2.7.7. Protein evaluation. Bovine serum albumin (BSA) was used as a standard to measure the protein as per method reported by Bradford (1976).

2.2.8. Evaluation of infarct volume

The male rats were sacrificed after 2.0 h MCAO followed by 22.0 h reperfusion effectively and the take-off the brain and placed in the brain matrix. In short, 1.50 milli meter coronal sections of brain were cut by the pointed blades. These brain sections were

stained by the 0.100% triphenyl tetrazolium chloride (TTC) in which normal saline used as a diluting solvent at 37.0 ± 1.0 °C for 15.0 min. TTC is used as a proton-acceptor mainly for the pyridine nucleotide-linked dehydrogenase generally in which cytochromes were acts as a very essential role at the time of construction of the inner mitochondrial membrane and construction of the electron transport chain. The tetrazolium salt was reduced through the enzymes which are lipid soluble in formazan having red color. The best quality of scanner was used to scan high resolution sectioning of brain which contains a property that differentiate both types of tissues easily through their images scan as an intensed red stain for viable tissues and other without stained infarct tissues. The infarct volume was measured by the total calculated and average area of infarct volume from the both sides multiplied through thickness of the section. Infarct volume was added from every section and used for edema as mentioned as previously used by Ahmad et al., 2016b; Ahmad et al., 2019a.

2.2.9. Toxicity study

In vivo toxicity was performed to determine the mortality and histology after 14 days treatment. It was divided in different groups:

Group 1: SHAM (Normal Control) for rat's brain,
Group 2: SHAM + NE-gel + 0.50%CS (placebo or without NRG) for rat's brain,
Group 3: NRG-NE-gel + 0.50%CS for rat's brain,
Group 4: SHAM (Normal Control) for nasal mucosa,
Group 5: SHAM + NE-gel + 0.50%CS (placebo or without NRG) for nasal mucosa, and
Group 6: NRG-NE-gel + 0.50%CS for nasal mucosa

In brief, 50.0 mg NRG that should equivalent to 10 mg/kg was applied intranasally to the rats at one time every day morning (9.00 a.m.) upto 14 days. When we were going to give to other dose for the next dose application, we examined the every rat at every day and evaluate their behavior, morbidity, and mortality. Group 1 & 4 selected as normal control and untreated group. After completion of fourteen-days dosing; the rats were sacrificed to remove their brains as well as nasal mucosa. 10.0% Neutral-buffered formalin solution was fixed to the tissues sectioning along-with staining with hematoxylin and eosin. All the sectioning of histological changes was examined microscopically to compare the normal control group (Ahmad et al., 2016a).

2.3. Statistical analysis

All the experimental-results were evaluated as mean ± standard error of mean (SEM). Student's *t*-test was applied to calculate the statistical difference between two mean values for unpaired observations and examined through ANOVA i.e. Analysis of variance. The p-value was observed less than 0.05 and it was statistically significant.

3. Result

3.1. Naringenin-nanoemulsion preparation and their characterization

The globule-size and PDI of NRG-NE were documented as 91.39 ± 1.89 nm and 0.372 ± 0.014 respectively (Fig. 1A). NRG-NE + 0.50%CS pH were determined 4.51 ± 0.13.

3.2. In situ gel preparation and their characterization

Optimized-NRG-NE-gel + 0.50%CS was newly developed and shown as a clear and elegant in appearance. The assessment of newly Optimized-NRG-NE-gel + 0.50%CS was based upon the visual observation and it don't contained any entrapped globules or bubbles. On the basis of one year stability study of optimized-NRG-NE-gel + 0.50%CS, we didn't saw any type of separation in the phase, aggregation, and settling of this nanoformulation. All the characterization results were shown in the Table 1.

3.3. Gelation temperature

NRG-NE-gel + 0.50%CS have showed a conversion of sol to gel at 28.3 ± 1 °C (Table 1).

3.4. Hydrodynamic diameter, PDI, and zeta potential with SEM and TEM study

Optimized-NRG-NE-gel + 0.50%CS is a thermosensitive *in-situ* gel that was showed a globule-size and PDI i.e. 98.31 ± 1.17 nm and 0.386 ± 0.021 respectively (Fig. 1B). In the Fig. 1B was showed two different peaks which are related with globule-size. First Peak presented 97.20% intensity (SD ± 4.63) and all the globules were monodispersed at 98.31 nm. The other peak was shown 37.2 nm with 2.50% intensity. Zeta potential for optimized NRG-NE was – 19.24 mV but after the conversion of NRG-NE to NRG-NE-gel + 0.5%CS, ZP of NRG-NE-gel + 0.5%CS was found + 13.91 mV (Figure C). Zeta potential have shown positive results just because of the chitosan coated on *in situ* gel formation, it was also reported by Ahmad et al., 2017a; Ahmad et al., 2017b. We were also performed the TEM study for further confirmation of particle size for Naringenin Loaded nanoemulsion Naringenin (NRG-NE) (Fig. 1D), mucoadhesive Naringenin *in situ* gel based on chitosan [(NRG) – NE-gel + 0.5%CS] (Fig. 1E). In the both observations Fig. 1D & 1E, we found that the particle is<100 nm of both nanoformulations. Scanning Electron Microscopy (SEM) images of NRG-NE-gel + 0.5%CS have given us an idea about spherical and smooth surface of NRG-NE-gel + 0.5%CS particles (Fig. 1F) which is also confirmed by the TEM images (Fig. 1E). Fifty times dilutions have performed for the NRG-NE-gel + 0.5%CS for the TEM images as presented in Fig. 2. Polymeric micelles were aggregated and clearly shown in a broad view (Fig. 2A-1) on the basis of micrograph picture 2-A as scale was taken 500.0 nm). On the basis of another scale i.e. 100.0 nm, the most of the micelles were aggregates in which some of them were bigger and tiny particles (Fig. 2B). The bigger particles were showed in the Fig. 2B-1 which represents 75.38 nm and 97.98 nm in size. It can be NRG-NE suspended in the NRG-NE-gel + 0.5%CS system. The tiny-particles showed in the Fig. 2B-2 having 33.56 nm may be due to the Poloxamer-407 based polymeric-micelles.

3.5. The pH and viscosity of NRG-NE-gel + 0.5%CS

NRG-NE-gel + 0.5%CS was shown the viscosity i.e. 2447 ± 24 cp at 35.1 ± 1.0 °C and pH was noted 6.0 ± 0.20 (Table 1).

3.6. Determination of NRG-NE-gel retention studies for the nasal mucosa by CLSM

Disposition study of NRG-NE-gel + 0.5%CS was evaluated in the nasal mucosa by the identification of cross-sections of the nasal mucosa through CLSM-images. Goat-nasal mucosa was washed with buffer solution so many times in the presence of Cur-nanoemulsion for the different cross-sectioning of confocal images. Strong blue-coloured area was shown in the confocal images which
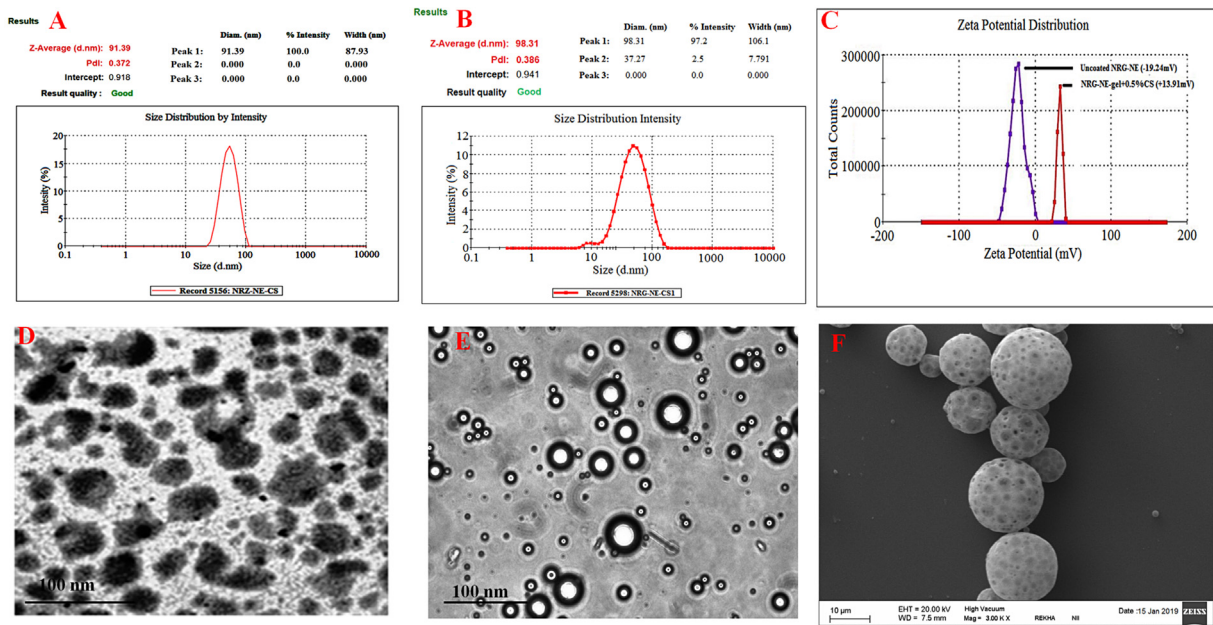
Fig. 1. Dynamic light scattering techniques for determining the particle size distribution of Naringenin (NRG)–NE **(A)** with NRG–NE–gel + 0.50%CS **(B)** & zeta potential **(D)**, TEM images for Naringenin Loaded nanoemulsion Naringenin (NRG–NE) **(D)**, mucoadhesive Naringenin (NRG)–NE–gel + 0.50%CS **(E)**, Scanning Electron Microscopy (SEM) **(F)** images of NRG–NE–gel + 0.50%CS.

Table 1
Optimized final nanoformulation of NRG-NE-gel + 0.50%CS.

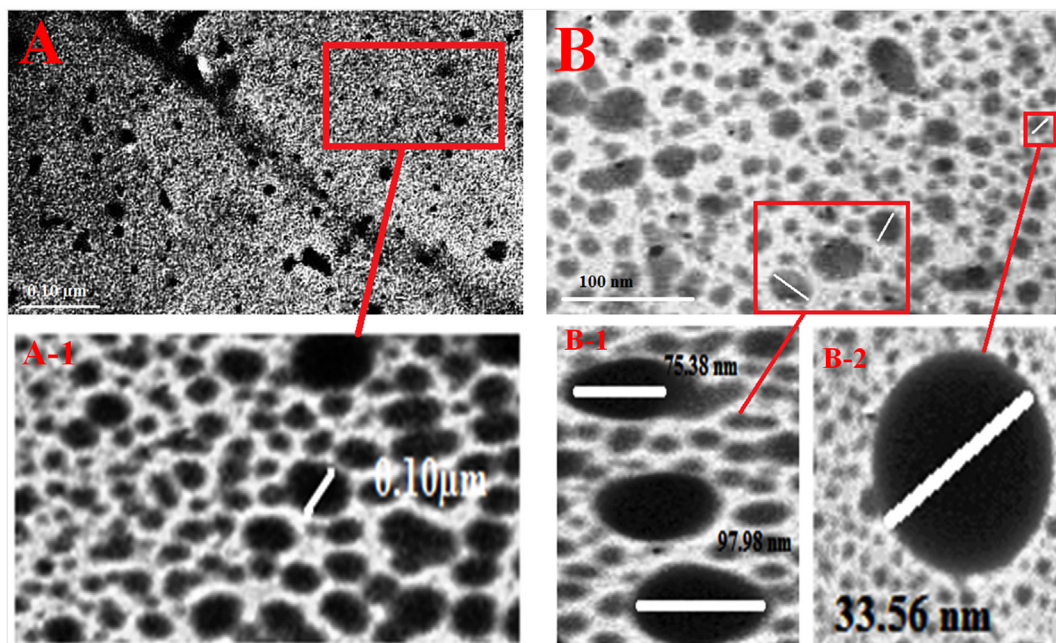| Gelation Temperature (°C)	pH	Viscosity (cp)	Firmness (g)	Consistency (g.sec)	Cohesiveness (g)	Index of Viscosity (g.sec)	Mucoadhesive Strength (Dynes/cm^2)
28.3 ± 1.0	6.0 ± 0.20	2447 ± 24	15.61	21.19	14.03	−8.75	6245.38

Fig. 2. Transmission electron microscopy images of Naringenin (NRG)-NE-gel + 0.50%chitosan after 50 times dilution (A) Nano-structural aggregates of polymeric micelles. Scale; 500 nm. (a-1) The enlarged view of **Fig.** A, showing a particle of 100 nm size present within the micellar aggregates. (B) Another field of the same sample with the scale of 100 nm, showing micellar aggregates, some larger and smaller particles.

was in-between and inside the nasal-mucosal-cells. NRG-NE-gel + 0.50%CS was exhibited very clear blue coloured due to their mucoadhesive nature in the Fig. 3B in which more intense area were compared to non-mucoadhesive Naringenin nanoemulsion-gel in the Fig. 3A.

3.7. In vitro NE–gel erosion evaluation

NRG-NE-gel and NRG–NE–gel + 0.50%CS were compared NE-gel erosion which is displayed in the Fig. 3C. NRG–NE–gel + 0.50%CS were eroded > 91.0% within 190.0 min and the erosion time of NRG-NE-gel was noted as 240.0 min.

3.8. NRG-permeation study by the use of bovine nasal mucosa

Fig. 3D represents the all different types of formulations *ex-vivo* permeation with their comparative permeation. NRG was permeated > 91.0% from the NRG-NE via goat-nasal-mucosa in 8.0 h while Naringenin was permeated 92.72 ± 6.41% from NRG–NE–gel + 0.50%CS in 12.0 h. NRG-suspension was determined the total permeation i.e. 36.14 ± 3.61% in 12.0 h which is very low in comparison of NRG–NE–gel + 0.50%CS and NRG-NE. For NRG–NE–gel

+ 0.50%CS, all permeation data were fitted to various kinetic models such as zero order, first order, Higuchi and Korsmeyer-Peppas at all time points. The value for R^2 was observed 0.9616, 0.9823, 0.9871 and 0.9653 respectively, while all the permeation data were fitted to the all same kinetic models.

3.9. UHPLC/ESI-Q-TOF-MS/MS based bioanalytical method development and their validation

NRG (analytes) and Quercetin (IS) of MS and MS-MS scans exhibited in Figs. 4 and 5. All the chromatograms acquired for blank brain homogenate [A], blank extracted plasma [B], extracted brain homogenate Naringenin (NRG) [C], plasma extracted Naringenin (NRG) [D], extracted brain homogenate Quercetin (QR) [E], plasma extracted Quercetin (QR) [F] have been presented in Fig. 6. Recovery (n = 6) has taken as mean i.e. > 78.99% from brain homogenates and plasma. The establish method was linear with $r^2 > 0.9992$ in brain homogenates and plasma in a range i.e. 1.0–2000.0 ng mL^{-1} for Naringenin (NRG) (Fig. 7). Blank plasma with blank brain homogenates chromatograms was determined for NRG to establish the selectivity for the developed method. Table 2 listed all the data related with the inter-day and intra-day preci-
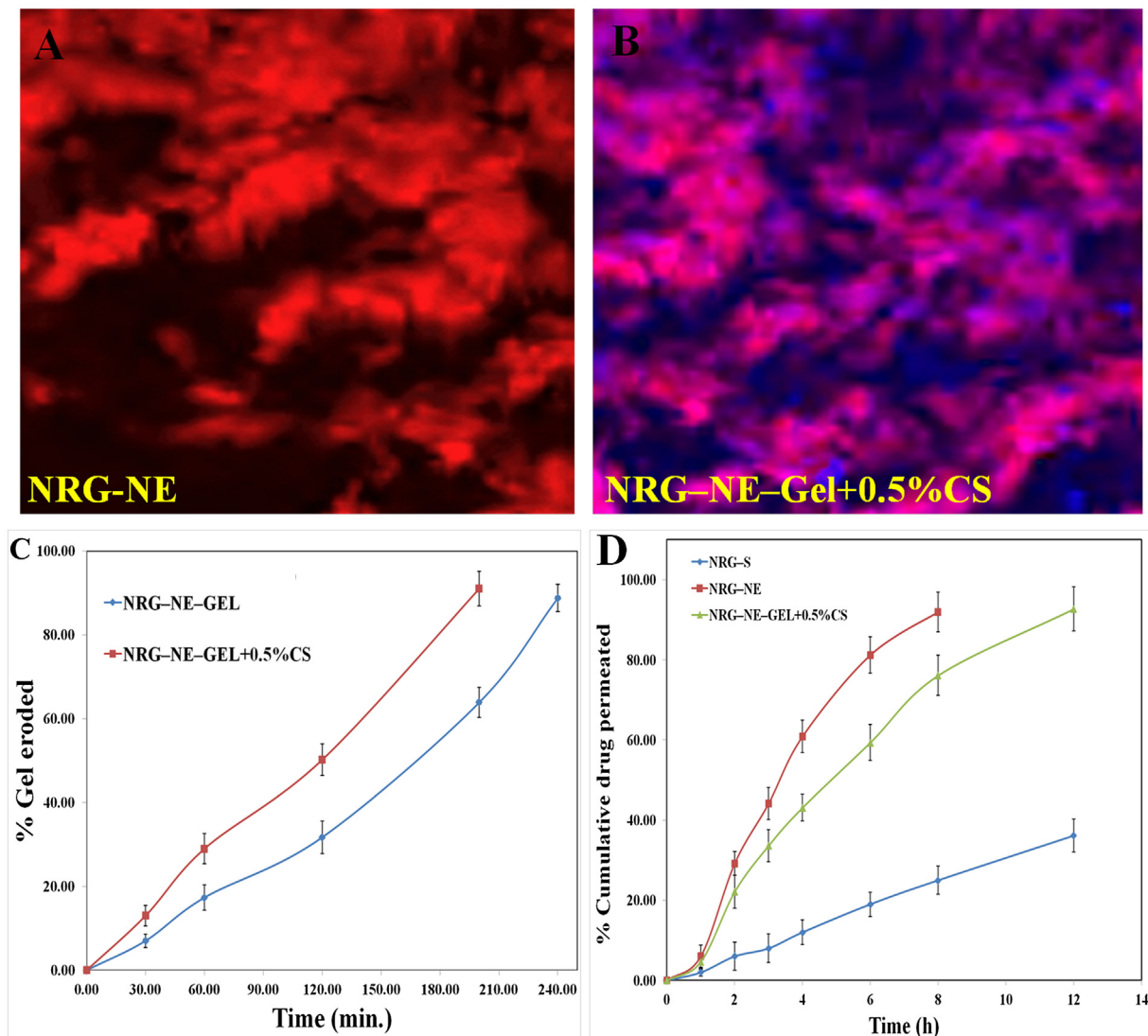

Fig. 3. CLSM images of Naringenin (NRG–NE) [A], mucoadhesive Naringenin (NRG)–NE-gel + 0.50%CS [B]. A comparative gel-erosion study of NRG–NE–gel, and NRG–NE–gel + 0.50%CS **[C]**. Comparative *ex-vivo* permeation profile of NRG-NE, NRG–NE–gel + 0.50%CS and Naringenin–suspension through goat nasal mucosa **[D]**.
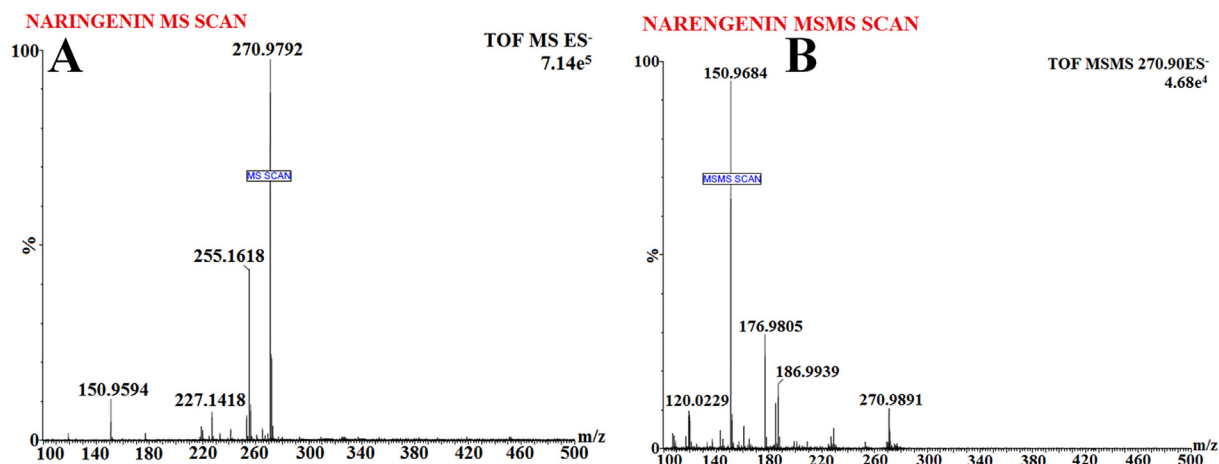
Fig. 4. Mass spectrum of **(A)** Naringenin parent ion (protonated precursor [M−H]⁻ ions at m/z: 270.9792) and **(B)** Naringenin product ion (major fragmented product ion at m/z 150.9684) showing fragmentation transitions.
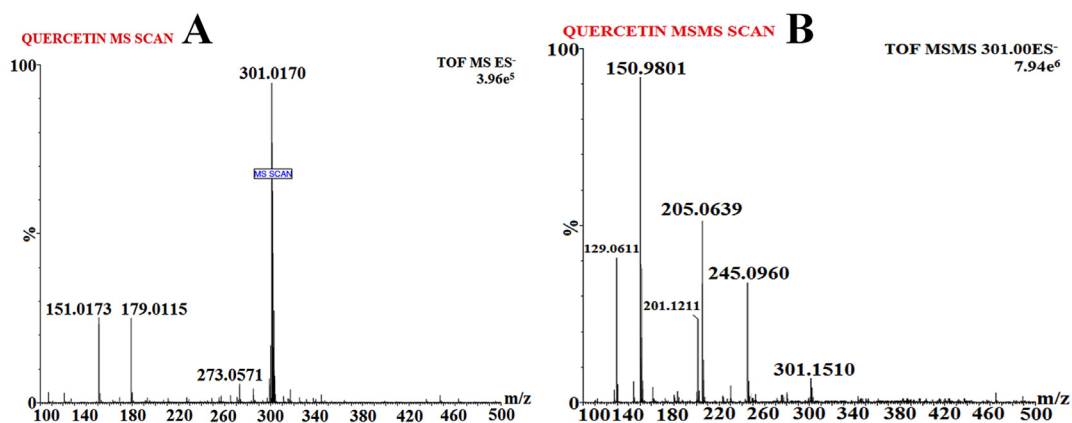

Fig. 5. Mass spectrum of, **(A)** Quercetin (IS) precursor ion (protonated precursor [M−H]⁻ ions at m/z 301.0170 and **(B)** IS product ion (major fragmented product ions at m/z 150.9801) showing fragmentation transitions.

sion and accuracy of optimized method. Finally, we acquired the data in-between 2.04 and 3.37%, 2.04–3.11%, and 1.01–3.23% for intra-batch and inter-batch percent precision of NRG to all QCs in lungs homogenate, brain homogenates and plasma. % Accuracy of all QCs for intra-batch and inter-batch were noted and it was within the range i.e. 95.10–99.00, 95.10–98.64 and 97.06–99.30% (Table 2). Freeze-thaw, long-term, post-processing, and bench-top stability for NRG were determined and established, all the data presented in the Table 3 for NRG was stable (Faiyazuddin et al., 2012).

3.10. Biodistribution, PK, %DTP, and %DTE

PK parameters was evaluated as AUC_{0-t}, T_{max}, C_{max}, K_e, and $t_{1/2}$ which were examined after the i.n. and i.v. application of NRG-NE-gel + 0.50%CS and their comparison to the pure NRG-Suspension (NRG-S) as shown in Table 4. All the data shown significantly improved the AUC_{0-t} after the optimized-NRG-NE-gel + 0.50%CS applications when we compare with the NRG-S in lungs, brain, and plasma of all these areas. NRG-concentration of brain and Brain/plasma ratio was determined maximum via i.n. as compared to i.v. administration in Table 5. Brain-bioavailability was significantly enhanced for newly optimized-NRG-NE-gel + 0.50%CS via i. v. route as compared to others with respect to %DTE, $AUC_{i.n}/AUC_{i.v.}$, and %DTP (Table 5, Fig. 8A).

3.11. Evaluation of pharmacodynamic parameters in ischemic brain

3.11.1. Evaluation of locomotor effect on rats

Evaluation of locomotor effect on each rat was examined for the duration of ten minutes. The locomotor effect was found to be significantly reduced ($p < 0.001$) in the MCAO's induced rats when it compared to controlled group (i.e. SHAM) in the Fig. 8B. It was also seen significantly enhancement in the locomotor activity for i.n. delivery of NRG-S and NRG-NE-gel + 0.50%CS (10.0 mg kg⁻¹ body weight) in comparison of MCAO's induced rats.

3.11.2. Evaluation of strength in the grip for rats

The grip strength was significantly reduced when compared with MCAO's induced rats to SHAM ($p < 0.001$). NRG-NE-gel + 0.50%CS (10.0 mg kg⁻¹ body weight) pretreated rats was determined were shown significantly enhanced the grip strength when it compared with MCAO-group ($p < 0.001$) (Fig. 8C).

3.11.3. Pretreatment-Naringenin effect on TBRAS level

The most important parameter is lipid peroxidation (LPO) and to evaluate the any deterioration due to in MCAO. Therefore, TBARS level was estimated and observed the Naringenin effect and it was found that significantly enhanced the TBARS-concentration ($p < 0.001$) when it compare to control (i.e. SHAM) group. Pretreated-NRG-rats (the dose: 10.0 mg kg⁻¹) reduced significantly
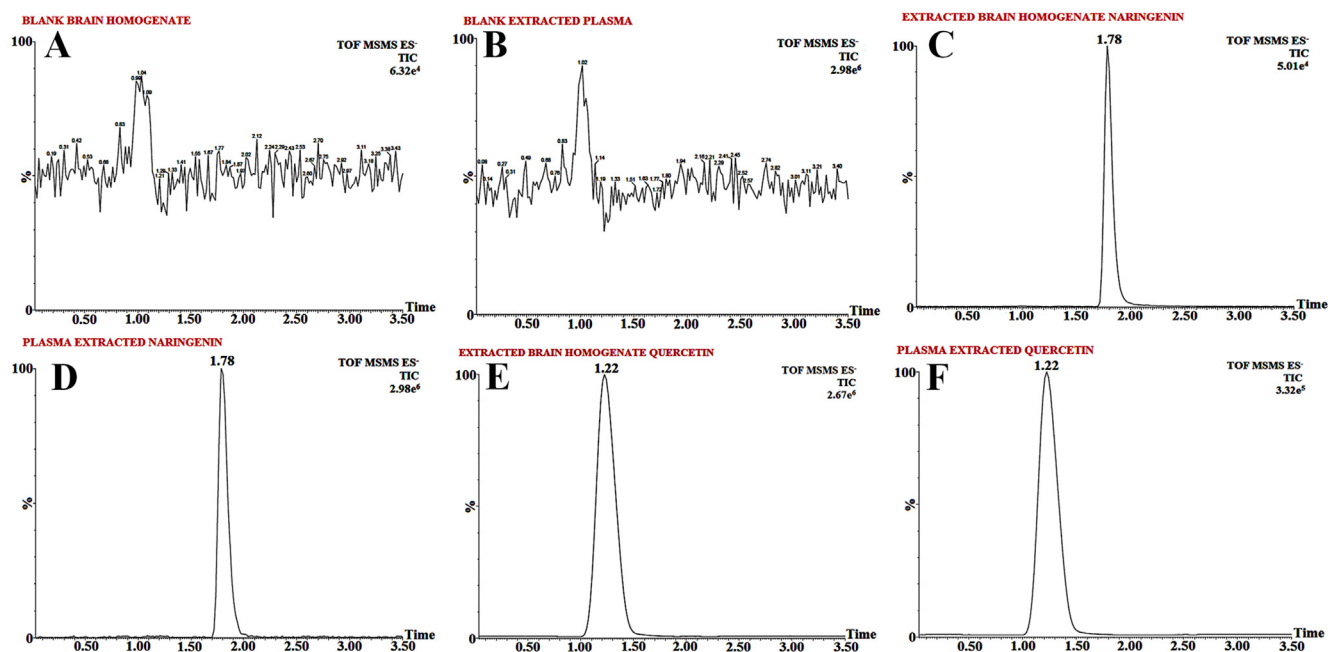
Fig. 6. Typical chromatograms of blank brain homogenate extracted **[A]**, blank extracted plasma **[B]**, extracted brain homogenate Naringenin **[C]**, Plasma Extracted Naringenin **[D]**, IS: extracted brain homogenate Quercetin **[E]**, and Plasma Extracted Quercetin **[F]**.

in TBARS-concentration when it compared to MCAO group rats (Fig. 8D). For the comparative effects for NRG-NE-gel + 0.50%CS (10.0 mg/kg body weight) showed the more significantly effects when it compared to NRG-S ($p < 0.001$).

3.11.4. Naringenin-effect on the system for endogenous-antioxidant action

Antioxidant enzymes like superoxide dismutase (SOD), Catalase, GPx, and GR reduced significantly for MCA-occluded rats when it compared to control group i.e. SHAM (Fig. 9). Pretreated-NRG-rats were shown the protective effects significantly as compared to MCAO-rats with NRG-NE-gel + 0.50%CS (10.0 mg/kg body weight; $p < 0.001$) and NRG-S ($p < 0.1$) (Fig. 9).

3.12. Naringenin-effect on infarction-volume through 2,3,5-Triphenyltetrazolium chloride (TTC)-stain

On the basis of infarction-images, NRG-S and NRG-NE-gel + 0.50%CS showed the protective results in the ischemic-brain. It was observed that the larger infarct volume significantly for MCAO-rats ($p < 0.001$) in comparison of SHAM-rats. From the MCAO-brain sectioning, the TTC-stain has given a reproducible and simply-visible infarction-area in the middle cerebral artery supplied areas after twenty-hours of reperfusion (Fig. 10A). All the TTC-stain brain images and infarction area measurement data were presented in the Fig. 10A & 10B for the different groups of MCAO + NRG-NE-gel + 0.50%CS, NRG-S, and MCAO with control (i.e. SHAM). The characteristic infarction area of MCAO was compared to control (i.e. SHAM) group. Pretreatment with NRG-S and NRG-NE-gel + 0.50%CS have shown the results that they reduced the infarct volume significantly with the comparison of MCAO-group. Although, MCAO + NRG-S group together-with MCAO + NRG-NE-gel + 0.50%CS group have showed a significant decrement (*$p < 0.05$, **$p < 0.01$) in tissue injury when it compared to MCAO-group.

3.13. Determination of toxicological response by the optimized-NRG-NE-gel + 0.50%CS

There was no toxicological response were not found in terms of mortalities for the all groups evaluation after the fourteen days study. We have not found any change morphologically i.e. in the microstructure of brain as well as nasal mucosa tissues when it was compared to control (i.e. SHAM) group of rats after the administration of NE-gel + 0.50%CS (placebo), and NRG-NE-gel + 0.50%CS (treatment). We were not found any visual signs in terms of inflammatory or necrosis point of view. The abovementioned results give us an idea about the safety of the optimized-NRG-NE-gel + 0.50%CS (Fig. 11). Finally, the toxicity studies showed the results for the safe nature of optimized-NRG-NE-gel + 0.50%CS.

4. Discussion

Ahmed et al. (2018) reported that the viscosity as well as concentration of Poloxamer increased; there was no change in the mucoadhesive strength of a poloxamer based any formulation. Thus here in this study, 0.50%w/v CS was used for the final optimized-NRG-NE-gel + 0.50%CS. In situ gel is performed very well in terms of gelation at the temperature in-between 25.0 and 34.0 °C. The problems related with manufacturing or administration or handling can comes when the use of gelation-temperature is < 25.0 °C. If the gelation temperature is > 34.0 °C, possibility of nasal cavity can gives us appositively-affects in the transition of sol to gel (Cho et al., 2011). We kept the gelation-temperature within the range for our optimized-NRG-NE-gel + 0.50%CS.

Polydispersity index of optimized-NRG-NE-gel + 0.50%CS was found to slightly more which may be due to two different sizes of globules peaks exhibited in the in situ-gel (Fig. 1B). It is recommend i.e. 97.2% particles were one size another 2.5% particles are very small. Therefore, we concluded our nanoformulation have two different sizes of particles. But all the particles are < 100.0 nm. But we didn't find any aggregation of the nanoparticles of the optimized-NRG-NE-gel + 0.50%CS. Poloxamer-407 based free poly-
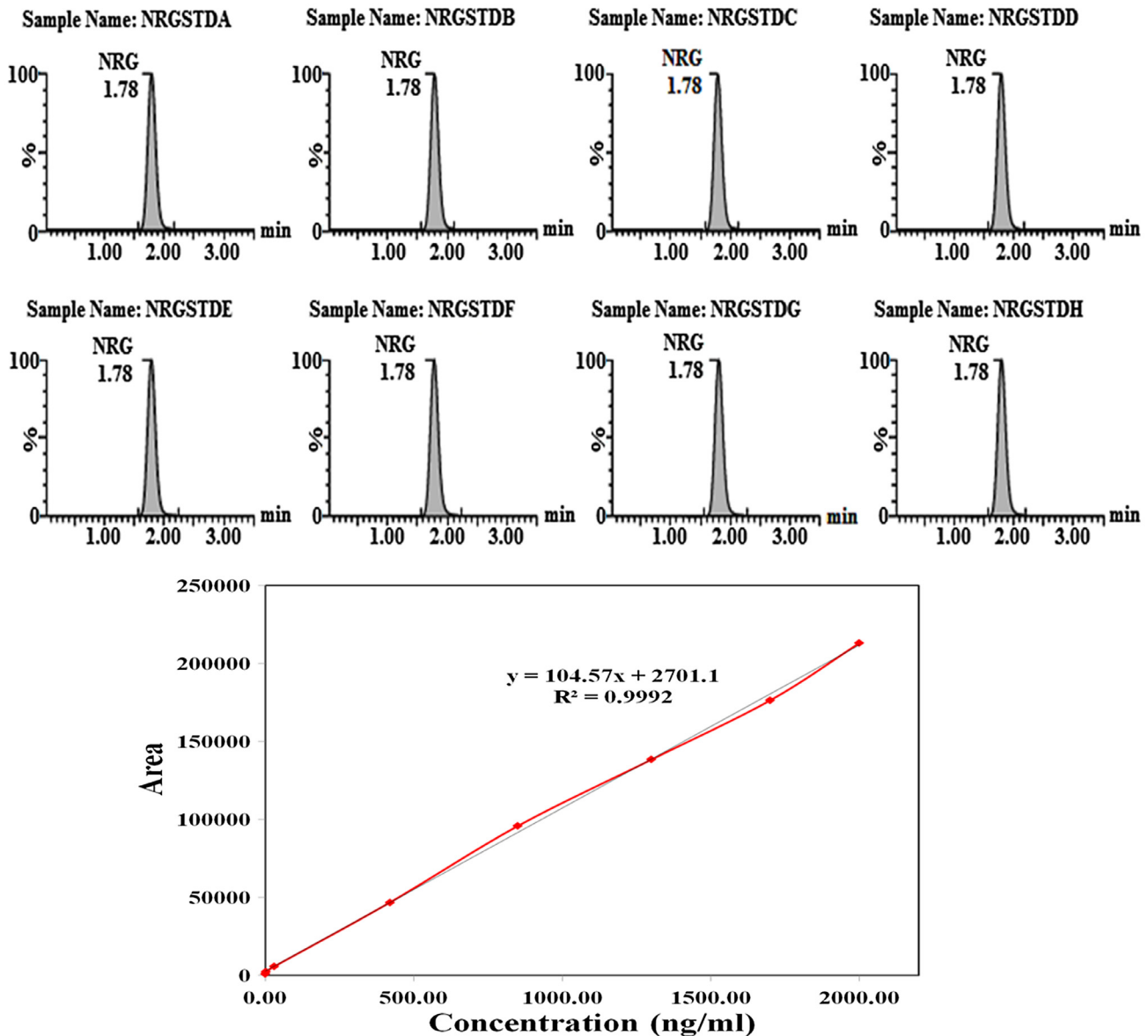
Fig. 7. Calibration standard (Naringenin) peaks at different calibration standards 1.0; 2.0; 31.0; 420.0; 850.0; 1300.0; 1700.0; and 2000.0 ng/ml with their calibration curve graph (1.00 to 2000.00 ng/ml).

meric micelles showed one peak. Possibility of another peak shown in the sample may be due to the presence of NRG-NE. Additionally, optimized-NRG-NE-gel + 0.50%CS were diluted hundred times before going to the analysis of globule size. Thus it has been given a clear idea about two different sizes of particles present in the optimized-NRG-NE-gel + 0.50%CS.

At the end, we performed the TEM-analysis that proved us very little amount of the particles are also present due to the presence of NRG-NE which is less than 2.2% in the optimized *in situ* NRG-NE-gel + 0.50%CS and it also confirmed that in optimized-gel, there was no aggregation of particles. It was concluded the stability of optimized-*in situ*-NRG-NE-gel + 0.50%CS (Fig. 2) (Napper et al., 1971). Mucoadhesive potency of optimized-NRG-NE-gel + 0.50% CS is due to the presence of the CS. It will be benefitted to enhance the permeation time and mucociliary retention time. On the basis of mucoadhesive strength test for optimized-NRG-NE-gel + 0.50% CS was within the limit as reported by the Singh et al., 2013 that maximum limit should be less than 10,000.0 dynes cm^{-2} for the nasal mucosal membrane.

Optimized-NRG-NE-gel + 0.50%CS contained enough cohesiveness, consistency, and firmness to survive opposite the ciliary movement. The viscosity index is the most important parameter to measure the effect of temperature on optimized-gel. If the viscosity index is maximum then temperature-dependent alteration in viscosity is lower. It is vice versa effect. NRG-NE-gel + 0.50%CS resulted lower viscosity-index i.e. −8.75 that can be maximum sensitive to alter in the temperature. If the NRG-NE-gel + 0.50%CS have high viscosity that is thought to be enhance the contact time between NRG and mucosal membrane. Finally it can be increase the permeation time. The pH of optimized-*in situ*-NRG-NE-gel + 0.50%CS was observed that the pH was also important parameter for the intranasal administration of optimized-*in situ*-NRG-NE-gel + 0.50%CS. Nasal cavity contained a pH limit-range 5.50 to 6.50 thus our optimized-*in situ*-NRG-NE-gel + 0.50%CS have comes under this limit range for the nasal compatibility (Arora et al., 2002).

NRG–NE–gel + 0.5%CS illustrated a quick gel-erosion i.e. > 91.01% within 3.33 h. From the published literature, Wang et al,

Table 2
Precision and Accuracy Data for Naringenin in different Biomatrixes.

Biomatrix	Quality Controls Samples	Theoretical Concentration (ng mL^{-1}) or (ng g^{-1})	Intra-batch precision			Inter-batch precision			Recovery[c] (%)
			Observed Concentration (ng mL^{-1}) or (ng g^{-1}) ± S.D.	Accuracy[a] (%)	Precision[b] (%C.V.)	Observed Concentration (ng mL^{-1}) or (ng g^{-1}) ± S.D.	Accuracy[a] (%)	Precision[b] (%C.V.)	
Brain Homogenate	LOQQC	1.02	0.98 ± 0.02	96.08	2.04	0.97 ± 0.03	95.10	3.09	80.91
	LQC	3.00	2.89 ± 0.09	96.33	3.11	2.88 ± 0.08	96.00	2.78	81.62
	MQC	810.00	792.01 ± 24.16	97.78	3.05	790.82 ± 23.87	97.63	3.02	79.27
	HQC	1600.00	1578.23 ± 41.23	98.64	2.61	1576.02 ± 39.02	98.50	2.48	82.56
Lungs Homogenate	LOQQC	1.02	0.97 ± 0.03	95.10	3.09	0.98 ± 0.02	96.08	2.04	79.97
	LQC	3.00	2.97 ± 0.10	99.00	3.37	2.96 ± 0.09	98.67	3.04	80.07
	MQC	810.00	786.01 ± 23.17	97.04	2.95	784.20 ± 24.62	96.81	3.14	81.02
	HQC	1600.00	1579.99 ± 39.04	98.75	2.47	1574.27 ± 40.18	98.39	2.55	78.99
Plasma	LOQQC	1.02	0.99 ± 0.03	97.06	3.03	1.00 ± 0.02	98.04	2.00	80.63
	LQC	3.00	2.97 ± 0.04	99.00	1.35	2.96 ± 0.03	98.67	1.01	81.04
	MQC	810.00	795.02 ± 25.65	98.15	3.23	791.53 ± 23.98	97.72	3.03	80.48
	HQC	1600.00	1588.84 ± 40.26	99.30	2.53	1584.28 ± 39.10	99.02	2.47	81.79

Values (Mean ± SD) are derived from 6 replicates: [a]Accuracy (%) = Mean value of [(mean observed concentration)/(theoretical concentration)] × 100; [b]Precision (%): Coefficient of variance (percentage) = standard deviation divided by mean concentration found × 100; [c]Recovery (%) = Mean value of (peak height (mV) obtained from extracted biological sample)/(peak height (mV) obtained from aqueous sample) × 100.

Table 3
Validation: Stability Data for Naringenin in different Biomatrixes.

Exposure condition	LQC(3.0 ng/mL or ng g^{-1})			MQC(810.0 ng/mL or ng g^{-1})			HQC (1600.0 ng/mL or ng g^{-1})		
	Brain Homogenate	Lungs Homogenate	Plasma	Brain Homogenate	Lungs Homogenate	Plasma	Brain Homogenate	Lungs Homogenate	Plasma
Long term stability; recovery (ng) after storage (-80 ± 2 °C)									
Previous day	2.99 ± 0.01	2.98 ± 0.02	2.96 ± 0.03	804.61 ± 25.41	799.01 ± 21.01	801.01 ± 22.11	1592.01 ± 35.01	1590.11 ± 34.72	1591.72 ± 32.87
30th Day	2.91 ± 0.02 (97.32%)	2.89 ± 0.02 (96.98%)	2.87 ± 0.02 (96.96%)	781.24 ± 24.78 (97.10%)	777.98 ± 23.91 (97.37%)	781.04 ± 21.03 (97.51%)	1578.11 ± 29.26 (99.13%)	1578.29 ± 34.11 (99.26%)	1577.25 ± 32.41 (99.09%)
Freeze–thaw stress; recovery (ng) after freeze–thaw cycles (-80 °C to 25 ± 1 °C)									
Pre-Cycle	2.97 ± 0.01	2.98 ± 0.01	2.96 ± 0.02	806.02 ± 24.16	803.27 ± 22.26	801.81 ± 22.83	1590.93 ± 35.19	1588.38 ± 33.27	1590.27 ± 33.61
First Cycle	2.92 ± 0.02 (98.32%)	2.90 ± 0.02 (97.32%)	2.88 ± 0.01 (97.30%)	792.11 ± 23.24 (98.27%)	795.37 ± 23.34 (99.02%)	791.27 ± 23.02 (98.69%)	1587.97 ± 34.27 (99.81%)	1580.27 ± 34.00 (99.49%)	1579.89 ± 32.87 (99.35%)
Second Cycle	2.86 ± 0.03 (96.30%)	2.83 ± 0.03 (94.97%)	2.77 ± 0.02 (93.58%)	784.67 ± 22.01 (97.35)	783.81 ± 21.28 (97.58%)	782.01 ± 21.89 (97.53%)	1578.12 ± 33.91 (99.19%)	1572.50 ± 33.27 (99.00%)	1570.44 ± 30.04 (98.75%)
Third Cycle	2.78 ± 0.02 (93.60%)	2.77 ± 0.02 (92.95%)	2.69 ± 0.03 (90.88%)	775.91 ± 23.72 (96.26%)	771.38 ± 23.04 (96.03%)	774.91 ± 24.03 (96.65%)	1570.03 ± 33.76 (98.69)	1565.92 ± 30.26 (98.59%)	1566.83 ± 29.68 (98.53%)
Bench top stability; recovery (ng) at room temperature (25 ± 2 °C)									
0 h	2.93 ± 0.02	2.95 ± 0.01	2.97 ± 0.03	804.92 ± 24.00	806.17 ± 22.45	803.20 ± 22.01	1588.83 ± 33.09	1599.26 ± 31.87	1591.71 ± 35.02
24 h	2.79 ± 0.02 (95.22%)	2.88 ± 0.2 (97.63%)	2.90 ± 0.02 (97.64%)	789.97 ± 22.56 (98.14%)	781.96 ± 21.01 (97.00%)	779.92 ± 20.01 (97.10%)	1572.75 ± 30.90 (98.99%)	1588.27 ± 29.93 (99.31%)	1569.01 ± 30.98 (98.57%)
Post processing stability; recovery (ng) after storage in auto sampler (4 ± 0.4 °C)									
0 h	2.96 ± 0.01	2.92 ± 0.02	2.89 ± 0.02	801.29 ± 21.98	799.92 ± 22.23	800.18 ± 22.23	1591.72 ± 32.54	1597.98 ± 33.01	1592.01 ± 33.28
4 h	2.77 ± 0.02 (93.58%)	2.81 ± 0.02 (96.23%)	2.76 ± 0.02 (95.50%)	788.01 ± 23.28 (98.34%)	779.87 ± 20.05 (97.49%)	788.91 ± 23.03 (98.59%)	1579.00 ± 30.89 (99.20%)	1581.17 ± 32.80 (98.95%)	1577.71 ± 31.81 (99.10%)

Values (Mean ± SD) are derived from six replicates. Figures in parenthesis represent analyte concentration (%) relative to time zero. Theoretical contents; LQC: 3.0 ng mL^{-1}; MQC: 810.0 ng mL^{-1}; and HQC: 1600.0 ng mL^{-1}.

Table 4
Pharmacokinetic profile of different formulations after dosing the Wistar rats intranasally and intravenously at the dose of 10 mg kg^{-1} in brain and plasma (n = 6, mean ± SD).

Formulation Administration	Samples	Cmax(ng/mL g)	Tmax	t$_{1/2}$ (h)	Ke (h^{-1})	AUC$_{0-t}$ (ng min/ml g)
NRG (i.n.)	Brain	91.82 ± 5.34	2.00	9.19 ± 0.83	0.07545 ± 0.00008	781.25 ± 22.17
	Plasma	21.71 ± 1.82	0.50	5.27 ± 0.43	0.13148 ± 0.00034	87.29 ± 4.84
NRG (i.v.)	Brain	46.18 ± 2.83	2.00	9.18 ± 0.74	0.07552 ± 0.00009	331.52 ± 11.15
	Plasma	609.79 ± 19.01	0.50	4.05 ± 0.33	0.17121 ± 0.00010	1630.75 ± 56.69
(NRG–NE–gel + 0.5%CS) i.n.	Brain	416.50 ± 12.01	2.00	22.42 ± 1.82	0.03092 ± 0.00007	5600.99 ± 144.92
	Plasma	91.27 ± 4.83	2.00	18.35 ± 0.97	0.03777 ± 0.00009	995.60 ± 24.59
(NRG–NE–gel + 0.5%CS) (i.v.)	Brain	178.92 ± 7.38	2.00	11.17 ± 0.88	0.06204 ± 0.00010	1884.75 ± 79.92
	Plasma	551.6 ± 19.11	1.00	6.79 ± 0.072	0.10204 ± 0.00021	4056.29 ± 117.13
NRG (i.n.)	Brain/Plasma	4.23	4.00	1.74	0.57	8.95
NRG (i.v.)	Brain/Plasma	0.076	4.00	2.27	0.44	0.20
(NRG–NE–gel + 0.5%CS) (i.n.)	Brain/Plasma	4.56	1.00	1.22	0.82	5.63
(NRG–NE–gel + 0.5%CS) (i.v.)	Brain/Plasma	0.33	2.00	1.65	0.61	0.47

Table 5
Drug Targeting Efficiency and Direct Nose-to-Brain Transport Following Intranasal Administration of different formulations.

Formulations	Drug Targeting Efficiency (%DTE)[*]	Direct Nose-to-Brain Transport (%DTP)[*]	Comparative Bioavailability[*] ($AUC_{i.n.}/AUC_{i.v.}$); (%)	
			Blood	Brain
NRG–NE–gel + 0.5%CS	1223.91 ± 69.25	99.47 ± 0.61	24.5 ± 0.20	297.1 ± 36.71

[*] Parameters are derived using mean ± SEM values of 6 different estimations.
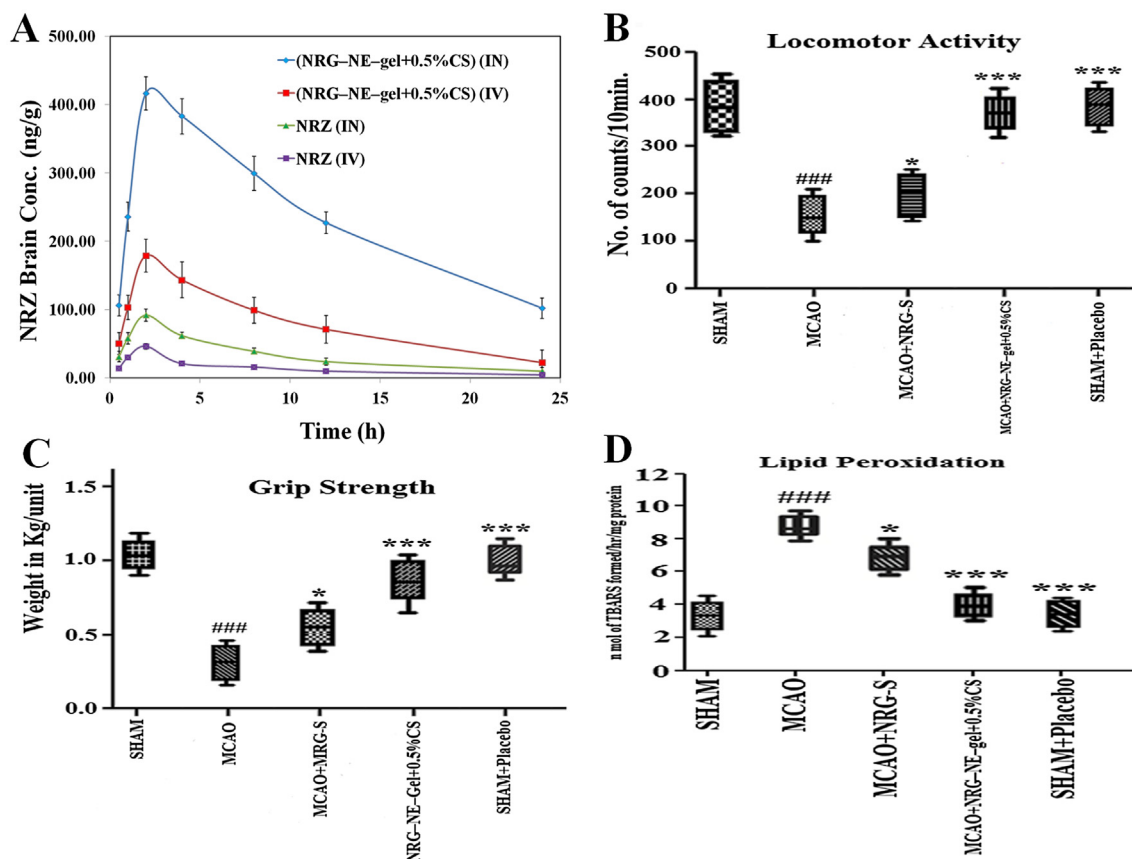
Fig. 8. Pharmacokinetic profiles of Naringenin concentration in brain at different time intervals after administration of optimized NRG–NE–gel + 0.50%CS compared with pure Naringenin **[A]**. Graph showing results of various groups treated with NRG–S, and NRG–NE–gel + 0.50%CS on locomotor activity, grip strength in middle cerebral artery–occluded (MCAO) rats. Data represented as mean ± SEM of six animals. Significance was determined as [###]$P < 0.001$ when compared with sham group; [*]$P < 0.05$, [***]$P < 0.001$ when compared with MCAO group **[B & C]**. Effect of NRG–NE–gel + 0.50%CS showed pre-treatment on TBARS content. TBARS content was significantly increased in MCAO group as compared to sham group. Significance was determined as [###]$P < 0.001$ when compared with sham group; [*]$P < 0.05$, [***]$P < 0.001$ when compared with MCAO group **[D]**.

2017b had been optimized an *in situ*-gel (S3) by the use of 20.50% Poloxamer-407, 3.30% Poloxamer-188, and 0.30% HPMC (for enhancement of mucoadhesion). They established 94.60 ± 5.80% gel-erosion within 6.0 h. This difference in erosion of gel may be due to the little bit acidic pH of the optimized-gel and it may be the presence of glacial acetic acid (Ur-Rehman et al, 2011).

From NRG-NE, NRG had showed the highest permeation in comparison of two formulations that was in dissolution form. The permeation of NRG from NRG-S was observed just opposite data. Optimized-*in situ*-NRG-NE-gel + 0.50%CS had shown permeation little bit smaller in comparison of NRG-NE. But it has been observed more satisfy permeation when it compare to NRG-S. The NRG-release and permeation showed Higuchi-kinetic-model ($R^2 = 0.9871$) from the planar-optimized-*in situ*-NRG-NE-gel + 0.50%CS that is suggested by Siepmann et al., 2001, it is a best example of diffusion-based-permeation followed by sink condition. Once the aqueous medium has come in contact to the gel, it forms the planar-layer of Poloxamer-407 after the dilution. The

gel is converted into sol form in the above mentioned layer when the Poloxamer-407 concentration has been diluted < 20.0% w/v. As a result, a free layer of NRG-NE was spread on the nasal mucosal layer. NRG permeated through the one-dimensional diffusion with an ideal sink condition.

Isopropyl Alcohol is a famous reference-irritant but Tween-80 concentration was used more than 10.0%w/w that showed the irritating or toxic effect. Same results were also shown on the gastrointestinal tract (Daher et al., 2003). In addition to micro/nanoemulsions prepared from Tween-80 were observed safe. But it was also reported for topical irritation and hypersensitivity. Hemolytic action was also reported with the Tween-80 using more than 80.0 μL/ml concentration (Kaur and Mehta, 2017). Tween-80 and PEG were taken ratio 4:1 for S_{mix} (10.0% v/v), here Tween-80 was taken 8.0% v/v. This concentration is considered as safe. When we prepared *in situ* hydrogel from NRG-NE after that the Tween-80 concentration was again reduced. Therefore, NRG-NE and NRG-NE-gel + 0.50%CS were not showed
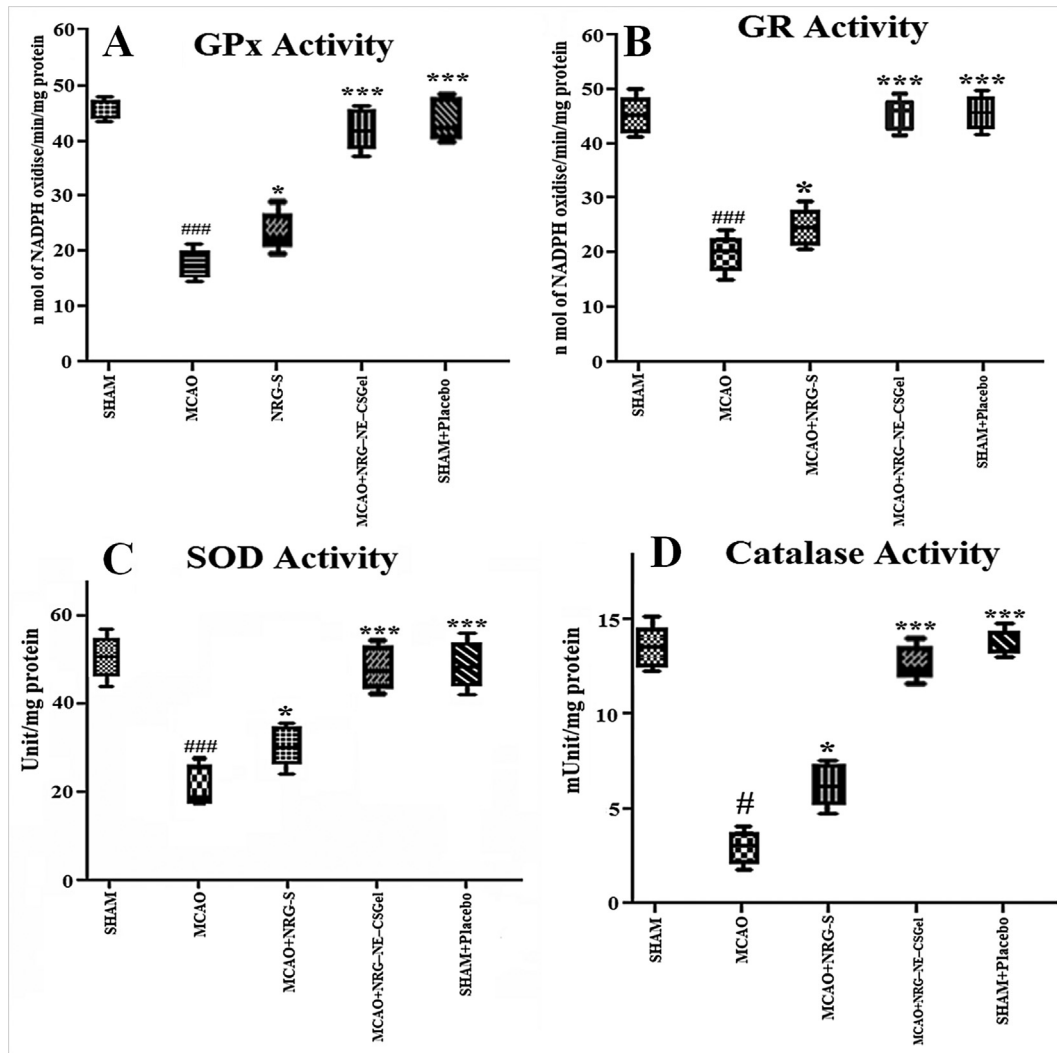
Fig. 9. Effect of NRG–NE–gel + 0.50%CS showed on the activity of various enzymes in different treated groups. Results were expressed as mean ± SEM of six animals. Significance was determined as $^{\#\#\#}P < 0.001$ when compared with sham group; $^*P < 0.05$, $^{***}P < 0.001$ when compared with MCAO group.
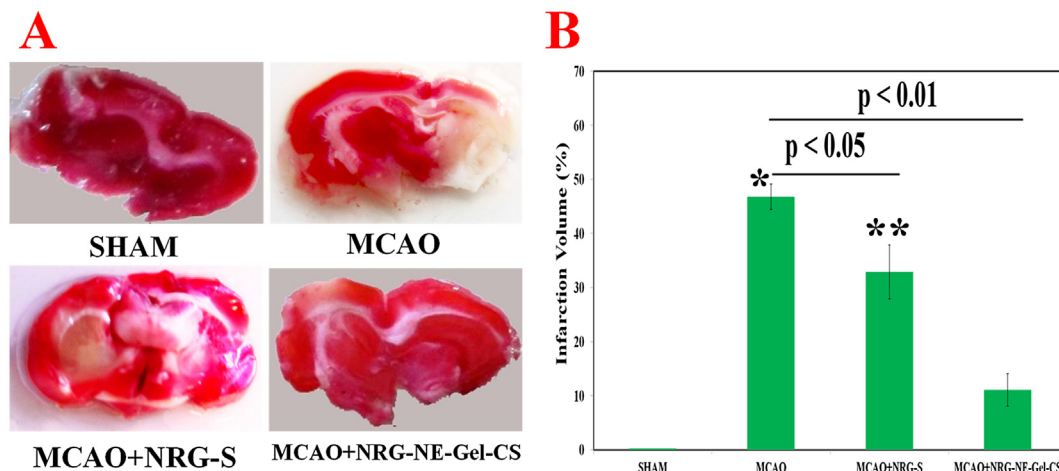

Fig. 10. [A] Representative photographs of brain sections stained with 0.1% TTC, and measurement of infarct volumes of MCAO, MCAO + NRG-S group, and NRG–NE–gel + 0.50%CS group are presented. MCAO group produced a significant lesion over SHAM group. **[B]** However, MCAO + NRG-S group and MCAO + NRG–NE–gel + 0.50%CS group showed a significant ($^*p < 0.05$; $^{**}p < 0.01$) reduction in tissue damage as compared to MCAO group.
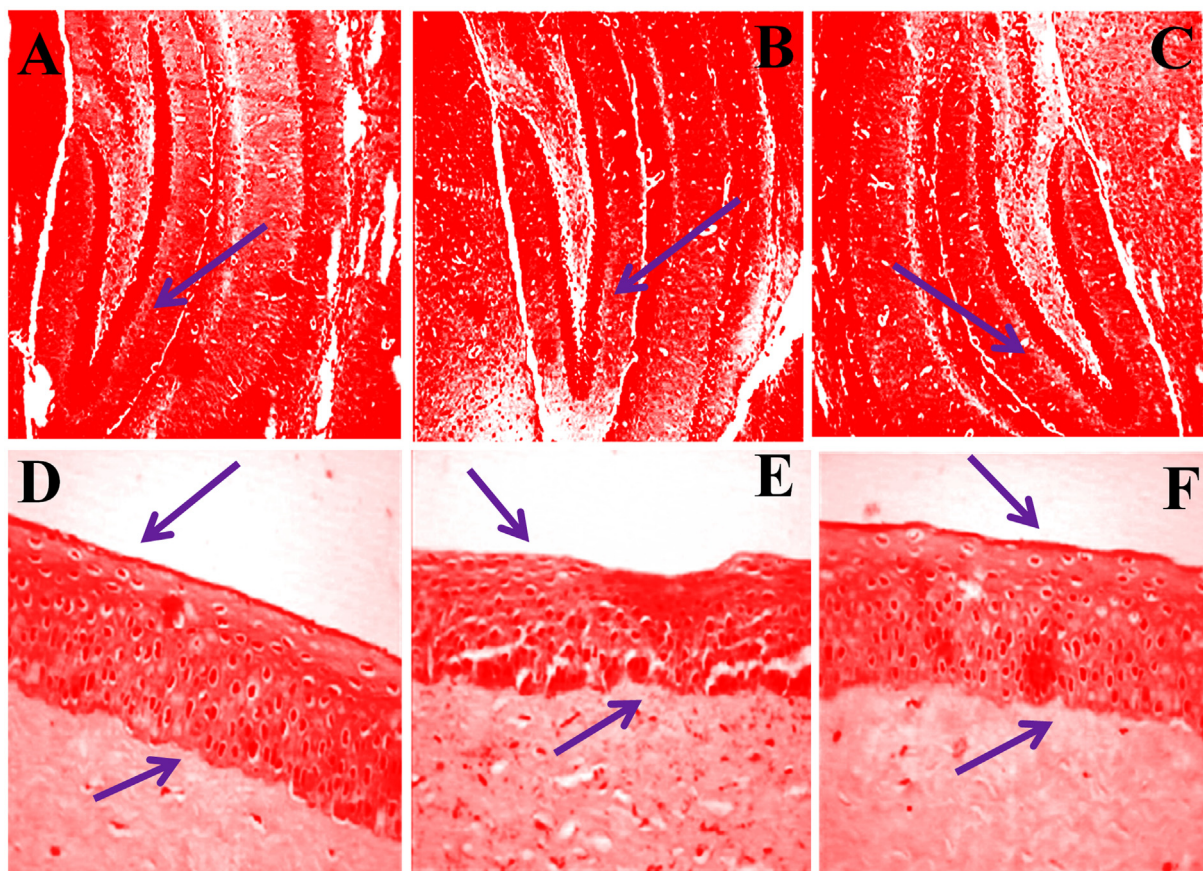
Fig. 11. Representative photomicrographs showing the TS of rats' brain (A, B, and C) and nasal mucosa (D, E, and F) for SHAM (Main control group), NE-gel + 0.50%CS (placebo), NRG-NE-gel + 0.50%CS treated groups, respectively after 14 days.

any toxic effects on the brain as well as nasal mucosa. Intranasal application of NRG-NE-gel + 0.50%CS in the rats have been repeated for fourteen days toxicity studies. There was no any sign of toxicity or any substantial inflammation. Therefore, optimized-NRG-NE and NRG-NE-gel + 0.50%CS is safe to be used for brain targeting (Fig. 11).

According to the US-FDA, 2018 bioanalytical guideline, Stability studies were performed and also calculated the % of remaining NRG in the optimized-NRG-NE-gel + 0.50%CS. All the factors related with optimized-NRG-NE-gel + 0.50%CS were also determined like active and inactive ingredients interactions, dosage form, pH of the dosage form, even the manufacturing processes, packaging materials etc. (Ahmad et al., 2016b). Rate constant were also determined i.e. 1.367×10^{-4} at 25.0 °C for optimized NRG-NE-gel + 0.50%CS. It was degraded slowly and it will be remained stable upto ~2.98 years. It showed a very minor effect on the optimized-NRG-NE-gel + 0.50%CS that is negligible (Ahmad et al., 2016b). Opt-NRG-NE-gel + 0.50%CS recommended more capable to the brain-delivery of NRG due to the presence of NRG as when compare to NE. Furthermore, CS as well as Tween-80 is renowned tight-junction opener. Therefore, they were enhanced NRG permeation paracellularly (Kaur and Mehta, 2017; Casettari L and Illum, 2014; Ahmad et al., 2016b).

Naringenin (NRG) is a flavorless, colorless flavanone, a type of flavonoid and also considered a low molecular weight compound, i.e. MW 272.257 with so many alcoholic groups present in the structure which imparts it the sensitivity to be easily detected in negative ion mode. Various solvents, i.e. methanol and isopropyl alcohol were tried for mobile phase selection but they didn't provide efficient chromatographic resolution. In addition, amongst

the buffer system studied, ammonium acetate (10.0%v/v) buffer system resulted in sharp peak and efficient signal response. Following different in-depth trials with change of solvents and buffer conditions etc., optimum chromatographic system for separation of NRG achieved was as follows: mobile phase: Acetonitrile (90.0%v/v): 2 mM Ammonium Acetate (10.0%v/v):Formic Acid (0.01%); flow rate: 0.25 ml/min and run time of 3.5 min (provided a baseline separation for NRG and IS without interference). The full-scan MS spectra for NRG revealed, protonated molecule at m/z 270.9792 as shown in Fig. 4A whereas, during direct infusion, IS mass spectra showed protonated molecule at m/z 301.0170 (Fig. 5A). The optimum collision energies employed were 19.39 eV (NRG) and 21.46 eV (QUR as IS) whereas capillary voltage of 21.0 and 3.0 kV were used in order to monitor precursor ions.

The biological sample preparation techniques most widely used are Protein precipitation (PPT), liquid–liquid extraction (LLE) and solid-phase extraction (SPE). In detail, initially PPT method was applied for method development but due to strong ion suppression of the endogenous substance in plasma, brain, and lungs homogenate. PPT separation was not considered further for NRG-separation. Although, aforementioned problem may be resolved with chromatographic separation but it will lead to run time sacrifice. Following different procedures, LLE method was finally found to be the efficient for preparing NRG brain and lungs homogenate samples. In order to achieve obtain optimum recovery, 7-organic extraction solvents were evaluated, i.e. ethyl acetate, chloroform, dichloromethane, acetonitrile, diethyl ether and tertiary butyl methyl ether (TBME), and n-hexane. To conclude, Ethyl Acetate yielded the highest recovery for the extraction of all matrixes which showed the highest recovery of > 79.27% for both NRG and

IS. Fig. 6C with 6D & 6E with 6F represents chromatogram for brain-homogenate and plasma shows elution time at 1.78 min and 1.22 min, respectively.

$AUC_{Brain})_{i.n.}$ was significantly higher in comparison of $(AUC_{Brain})_{i.v.}$ indicating that intranasally highest amount of NRG reached to the brain in comparison of i.v. route. Naringenin showed >90.0% plasma protein binding by the administered intravenous route. Moreover, NRG-S was given through i.n. route. NRG was directly reaches to the brain bypassing hepatic metabolism through this route. Some amount of NRG was also remaining in the systemic circulation that also goes into the liver via hepatic artery and ultimately partially degraded.

Alternatively, NRG-NE-gel + 0.50%CS was administered intranasally to reached to the brain directly and steadily i.e. in the $T_{max} = 2.00$ h in comparison of intravenously. This is because of the insignificant amount of protein binding, hepatic metabolism avoided, smaller the elimination rate constant ($K_e = 0.03092$). AUC of NRG was found to be higher from this (i.e. i.n.) route. These results were supported to the previously published data by Ahmad et al. (2016b).

In the rat's brain, %DTE was greatly enhanced i.e. 1223.91 ± 69.25% with highly increment of %DTP i.e. 99.47 ± 0.61%. This is because of the fast erosion of NRG-NE-gel + 0.50%CS, more rapidly NRG-release from the gel, and greater permeation of NRG via olfactory epithelial layer. Moreover, it is concluded that the NRG-NE-gel + 0.50%CS was administered via intranasally, NRG reached freely to the brain in high quantity because of the very less quantity of protein binding. In comparison to the i.v. route when it was administered through i.v. route and the NRG reached to the very less amount due to the higher protein binding (i.e. 85.0 to 95.0%) (Hu et al., 201)).

Rats for SHAM (i.e. control, without NRG-NE-gel + 0.50%CS) group exhibited highly and significantly recovered for the potency of grip and locomotor activity on the other side very-little improvement of rats for MCAO-group. SHAM + Substantial (i.e. without NRG/Placebo) group showed that they don't have any toxic effect in the brain. NRG-NE-gel + 0.50%CS was given intranasally and they showed highly significant results in terms of improvement for locomotor activity and grip strength in comparison of NRG-S (Fig. 8B).

MCAO i.e. stroke model was developed on the wistar rat which imitates and inspect on the ischemic brain of human. The most important parameter i.e. free radical has played a greater role in the alteration of neurobehavioral responses in developed ischemic model through the oxidative stress (Fukui et al., 2002) followed by the reduction of neurobehavioral source result in the ischemic brain therefore, any alteration of locomotion and motor behavior coordination (Hunter et al., 1998). The toxicity from the vehicle (SHAM + Placebo) was not observed for the locomotor and grip strength performance. But it is found opposite to the MCAO group i.e. reduction coordination and locomotion both.

Earlier reported research data was published in which behavioral outcomes was improved after NRG treatments as an antioxidant. Neuroprotective effects from NRG are measured to be a potent antioxidant, supportive earlier studies (Raza et al., 2013; Bai et al., 2014; Wang et al., 2017a). NRG-NE-gel + 0.50%CS reduce lipid peroxidation as a strong anti-oxidative damage indicator. Therefore, it prevents the oxidative stress through various mechanisms that defeat pro-oxidants by scavenging the free radicals (Bhandari et al., 2018). Any change in biochemical reactions because of oxidative stress, was seen in the ischemic brain damage come across through intensed cell mechanisms like enzymatic and non-enzymatic reactions. The brain membranes which are richer in lipid were attacked by the reactive oxygen species (ROS). It caused LPO and threat to neuronal survival. On the other hand, any antioxidants like NRG were detoxifying the free radicals and reducing the LPO-level thus NRG prevents the cell-damage (Kale et al., 1999). Current study, we observed that increased the LPO (TBARS) concentration and also decreased the GSH concentration as earlier published reported data by Ahmad et al., 2013; Zafar et al. 2003. Therefore, they observed the antioxidant defenses due to in-between the interconnection if any one problem between these mechanisms can be disrupt the total microenvironment (Sun et al., 2009). The reperfusion due to the ischemia is a major reason for greater production of free radicals that helps in lipid membrane oxidative injury and decreased the concentration of GSH as well as reliant on the enzymes activity like SOD, GPx, and GR as published by Khuwaja et al. (2011). At the time of cerebral ischemia, the free radicals were mostly damaged the SOD which results the destruction of cells by the various ways. NRG–NE–gel + 0.5%CS has been given prophylactically before the cerebral ischemic-injury which exhibited a significant SOD-activity because of use of superoxide radical (O^{2-}) at the time of reperfusion of cerebral ischemia. SOD-level reduced with other biochemical-enzymes in the MCAO group but all biochemical-enzymes and SOD do not affected due to the a protective role of NRG-NE-gel + 0.50%CS and even also seen i.e. not too much affected in the NRG-S group (less protective role due to the less amount of NRG-available) on the basis of clear identification of biochemical and histological data observation.

Infarction volume was measured with the help of the TTC stain which is a very important estimation for the ischemic stroke. It identified the many neuronal injuries as well as neurological destruction with the help of morphological-determination of infarction sizes in the brain-tissues after the brain-ischemic-injury (Bederson et al., 1986). In the MCAO group contained a very clear infarction and other behavioral alteration. If this group were treated by the NRG-NE-gel + 0.50%CS i.e. NRG decreased the infarct size with improved the behavioral-activity. Finally it is concluded; NRG-NE-gel + 0.50%CS and NRG-S have showed the decrement of the infarct size with improvement of the behavioral-activity Fig. 10A & B (Ahmad et al., 2017a). There was no alteration or not any toxic effects in the NE-gel + 0.50%CS (i.e. placebo) + SHAM (i.e. pretreated/substantial control)-group and the sham (i.e. control)-group. TTC stain is very helpful to determine and evaluation of the brain sectioning of SHAM (i.e. control) group, MCAO, NRG-NE-gel + 0.50%CS, and substantial-control group (i.e. SHAM + Placebo) in the Middle-cerebral-artery supplied (after the 22.0 h reperfusion) areas (Fig. 10).

5. Conclusion

Here we have reported in this study, the preparation of NE and conversion of mucoadhesive-NE and finally, the conversion of *in situ* gel which is based on the thermoresponsive for NRG. Opt-NRG-NE-gel + 0.50%CS have confirmed quick erosion of gel and permeation of NRG in the nasal mucosa. Bioanalytical method was developed and validated successfully on the very sensitive-system i.e. UHPLC/ESI-Q-TOF-MS/MS. This method was used successfully for the determination of PK and biodistribution-studies and the results showed the enhancement of brain-bioavailability by the i.n. application of Opt-NRG-NE-gel + 0.50%CS. In conclusion, NRG has been used for cerebral ischemia treatment effectively with decreasing the systemic side effects and finally complete study showed a strong neuroprotective drug against the oxidative stress and cellular damage. Furthermore, Opt-NRG-NE-gel + 0.50% CS were safe and useful on the basis of toxic studies results. Finally the major conclusion of our research study; Opt-NRG-NE-gel + 0.5%CS is new, a very effective role, non-invasive and can be safely targeted NRG-delivery to the brain for treatment of cerebral ischemia. But it is very important to perform in-depth pre-clinical and clinical studies for the before commercialization of Opt-NRG-

NE-gel + 0.50%CS in future which is based on the low risk/high benefit ratio.

Author's conflict

All authors don't contain any conflict amongst them.

Funding

Acknowledgments

References

Agrawal, A.K., Gupta, P.N., Khanna, A., Sharma, R.K., Chandrawanshi, H.K., Gupta, N., Patil, U.K., Yadav, S.K., 2010. Development and characterization of in situ gel system for nasal insulin delivery. Pharmazie 65 (3), 188–193. https://doi.org/10.1691/ph.2010.9188.

Ahmad, N., Ahmad, R., Al-Qudaihi, A., Alaseel, S.E., Fita, I.Z., Khalid, M.S., Pottoo, F.H., 2019. Preparation of a novel curcumin nanoemulsion by ultrasonication and its comparative effects in wound healing and the treatment of inflammation. RSC Adv. 9 (35), 20192–20206. https://doi.org/10.1039/c9ra03102b.

Ahmad, N., Ahmad, I., Umar, S., Iqbal, Z., Samim, M., Ahmad, F.J., 2016a. PNIPAM nanoparticles for targeted and enhanced nose-to-brain delivery of curcuminoids: UPLC/ESI-Q-ToF-MS/MS-based pharmacokinetics and pharmacodynamic evaluation in cerebral ischemia model. Drug Deliv. 23 (7), 2095–2114. https://doi.org/10.3109/10717544.2014.941076.

Ahmad, N., Ahmad, R., Naqvi, A.A., Ashafaq, M., Alam, M.A., Ahmad, F.J., Al-Ghamdi, M.S., 2017a. The effect of safranal loaded mucoadhesive nanoemulsion on oxidative stress markers in cerebral ischemia. Artif. Cells Nanomed. Biotechnol. 45 (4), 775–787. https://doi.org/10.1080/21691401.2016.1228659.

Ahmad, N., Ahmad, R., Alam, M.A., Ahmad, F.J., Amir, M., 2018a. Impact of ultrasonication techniques on the preparation of novel Amiloride-nanoemulsion used for intranasal delivery in the treatment of epilepsy. Artif. Cells Nanomed. Biotechnol. 46 (sup3), S192–S207. https://doi.org/10.1080/21691401.2018.1489826.

Ahmad, N., Ahmad, R., Alam, M.A., Ahmad, F.J., 2018b. Quantification and brain targeting of eugenol-loaded surface modified nanoparticles through intranasal route in the treatment of cerebral ischaemia. Drug Res (Stuttg). 68 (10), 584–595. https://doi.org/10.1055/a-0596-7288.

Ahmad, N., Ahmad, R., Naqvi, A.A., Alam, M.A., Ashafaq, M., Rub, R.A., Ahmad, F.J., 2018c. Intranasal delivery of quercetin-loaded mucoadhesive nanoemulsion for treatment of cerebral ischaemia. Artif. Cells Nanomed. Biotechnol. 46 (4), 717–729. https://doi.org/10.1080/21691401.2017.1337024.

Ahmad, N., Ahmad, R., Naqvi, A.A., Alam, M.A., Ashafaq, M., Samim, M., Iqbal, Z., Ahmad, F.J., 2016b. Rutin-encapsulated chitosan nanoparticles targeted to the brain in the treatment of Cerebral Ischemia. Int. J. Biol. Macromol. 91, 640–655. https://doi.org/10.1016/j.ijbiomac.2016.06.001.

Ahmad, N., Umar, S., Ashafaq, M., Akhtar, M., Iqbal, Z., Samim, M., Ahmad, F.J., 2013. A comparative study of PNIPAM nanoparticles of curcumin, demethoxycurcumin, and bisdemethoxycurcumin and their effects on oxidative stress markers in experimental stroke. Protoplasma 250, 1327–1338. https://doi.org/10.1007/s00709-013-0516-9.

Ahmad, N., Ahmad, F.J., Bedi, S., Sharma, S., Umar, S., Ansari, M.A., 2019. A novel nanoformulation development of Eugenol and their treatment in inflammation and periodontitis. Saudi Pharm. J. 27 (6), 778–790. https://doi.org/10.1016/j.jsps.2019.04.014.

Ahmad, N., Ahmad, R., Alam, M.A., Ahmad, F.J., Rub, R.A., 2018d. Quantification and evaluation of glycyrrhizic acid-loaded surface decorated nanoparticles by UHPLC-MS/MS and used in the treatment of cerebral ischemia. Curr. Pharm. Anal. 14, 1–15. https://doi.org/10.2174/1573412914666180530073613.

Ahmad, N., Al-Subaiec, A.M., Ahmad, R., Sharma, S., Alam, M.A., Ashafaq, M., Rub, R.A., Ahmad, F.J., 2019. Brain-targeted glycyrrhizic-acid-loaded surface decorated nanoparticles for treatment of cerebral ischaemia and its toxicity assessment. Artif. Cells Nanomed. Biotechnol. 47 (1), 475–490. https://doi.org/10.1080/21691401.2018.1561458.

Ahmad, N., 2017b. Rasagiline-encapsulated chitosan-coated PLGA nanoparticles targeted to the brain in the treatment of parkinson's disease. J. Liq. Chromatogr. Relat. Technol. 40 (13), 677–690. https://doi.org/10.1080/10826076.2017.1343735.

Ahmed, T.A., Badr-Eldin, S.M., Ahmed, O.A.A., Aldawsari, H., 2018. Intranasal optimized solid lipid nanoparticles loaded in situ gel for enhancing transmucosal delivery of simvastatin. J. Drug Deliv. Sci. Technol. 48, 499–508. https://doi.org/10.1016/j.jddst.2018.10.027.

Arora, P., Sharma, S., Garg, S., 2002. Permeability issues in nasal drug delivery. Drug Discov. Today 7 (18), 967–975. https://doi.org/10.1016/S1359-6446(02)02452-2.

Bai, X., Zhang, X., Chen, L., Zhang, J., Zhang, L., Zhao, X., Zhao, T., Zhao, Y., 2014. Protective effect of naringenin in experimental ischemic stroke: down-regulated NOD2, RIP2, NF-κB, MMP-9 and up-regulated claudin-5 expression. Neurochem. Res. 39 (8), 1405–1415. https://doi.org/10.1007/s11064-014-1326-y.

Barakat, S.S., Nasr, M., Ahmed, R.F., Badawy, S.S., Mansour, S., 2017. Intranasally administered in situ gelling nanocomposite system of dimenhydrinate: preparation, characterization and pharmacodynamic applicability in chemotherapy induced emesis model. Sci. Rep. 7 (1), 9910. https://doi.org/10.1038/s41598-017-10032-7.

Baranowska, I., Hejniak, J., Magiera, S., 2016a. Development and validation of a RP-UHPLC-ESI-MS/MS method for the chiral separation and determination of flavanone, naringenin and hesperetin enantiomers. Talanta 159, 181–188. https://doi.org/10.1016/j.talanta.2016.06.020.

Baranowska, I., Hejniak, J., Magiera, S., 2016b. Simultaneous Chiral Separation of Flavanone, Naringenin, and Hesperetin Enantiomers by RP-UHPLC-DAD. Chirality 28 (2), 147–152. https://doi.org/10.1002/chir.22559.

Bederson, J.B., Pitts, L.H., Germano, S.M., Nishimura, M.C., Davis, R.L., Bartkowski, H. M., 1986. Evaluation of 2,3,5-triphenyltetrazolium chloride as a stain for detection and quantification of experimental cerebral infarction in rats. Stroke 17 (6), 1304–1308. https://doi.org/10.1161/01.STR.17.6.1304.

Bhandari, R., Paliwal, J.K., Kuhad, A., 2018. Naringenin and its nanocarriers as potential phytotherapy for autism spectrum disorders. J. Funct. Foods. 47, 361–375. https://doi.org/10.1016/j.jff.2018.05.065.

Bonacucina, G., Misici-Falzi, M., Cespi, M., Palmieri, G.F., 2008. Characterization of micellar systems by the use of acoustic spectroscopy. J. Pharm. Sci. 97 (6), 2217–2227. https://doi.org/10.1002/jps.21156.

Bradford, M.M., 1976. A rapid and sensitive method for the quantitation of microgram quantities of protein utilizing the principle of protein-dye binding. Anal. Biochem. 72 (1–2), 248–254. https://doi.org/10.1016/0003-2697(76)90527-3.

Cabana, A., Ait-Kadi, A., Juhasz, J., 1997. Study of the gelation process of polyethylene oxidea -polypropylene oxideb -polyethylene oxidea copolymer (poloxamer 407) aqueous solutions. J. Colloid Interface Sci. 190 (2), 307–312. https://doi.org/10.1006/jcis.1997.4880.

Casettari, L., Illum, L., 2014. Chitosan in nasal delivery systems for therapeutic drugs. J. Control Release. 190, 189–200. https://doi.org/10.1016/j.jconrel.2014.05.003.

Cho, H.J., Balakrishnan, P., Park, E.K., Song, K.W., Hong, S.S., Jang, T.Y., Kim, K.S., Chung, S.J., Shim, C.K., Kim, D.D., 2011. Poloxamer/cyclodextrin/chitosan-based thermoreversible gel for intranasal delivery of fexofenadine hydrochloride. J. Pharm. Sci. 100 (2), 681–691. https://doi.org/10.1002/jps.22314.

Daher, C.F., Baroody, G.M., Howland, R.J., 2003. Effect of a surfactant, Tween 80, on the formation and secretion of chylomicrons in the rat. Food Chem. Toxicol. 41 (4), 575–582. https://doi.org/10.1016/S0278-6915(02)00299-5.

Faiyazuddin, M., Ahmad, N., Khar, R.K., Bhatnagar, A., Ahmad, F.J., 2012. Stabilized terbutaline submicron drug aerosol for deep lungs deposition: drug assay, pulmonokinetics and biodistribution by UHPLC/ESI-q-TOF-MS method. Int. J. Pharm. 434 (1–2), 59–69. https://doi.org/10.1016/j.ijpharm.2012.05.007.

Fakhari, A., Corcoran, M., Schwarz, A., 2017. Thermogelling properties of purified poloxamer 407. Heliyon. 3, (8). https://doi.org/10.1016/j.heliyon.2017.e00390 e00390.

Fukui, K., Omoi, N.O., Hayasaka, T., Shinnkai, T., Suzuki, S., Abe, K., Urano, S., 2002. Cognitive impairment of rats caused by oxidative stress and aging, and its prevention by vitamin E. Ann. N Y Acad. Sci. 959, 275–284. https://doi.org/10.1111/j.1749-6632.2002.tb02099.x.

Gratieri, T., Gelfuso, G.M., Rocha, E.M., Sarmento, V.H., de Freitas, O., Lopez, R.F., 2010. A poloxamer/chitosan in situ forming gel with prolonged retention time for ocular delivery. Eur. J. Pharm. Biopharm. 75 (2), 186–193. https://doi.org/10.1016/j.ejpb.2010.02.011.

Yan-Jun, Hu., Wang, Y., Ou-Yang, Y., Zhou, J., Liu, Y., 2010. Characterize the interaction between naringenin and bovine serum albumin using spectroscopic approach. J. Lumin. 130 (8), 1394–1399. https://doi.org/10.1016/j.jlumin.2010.02.053.

Hunter, A.J., Mackay, K.B., Rogers, D.C., 1998. To what extent have functional studies of ischaemia in animals been useful in the assessment of potential neuroprotective agents? Trends Pharmacol. Sci. 19 (2), 59–66. https://doi.org/10.1016/S0165-6147(97)01157-7.

Kale, M., Rathore, N., John, S., Bhatnagar, D., 1999. Lipid peroxidative damage on pyrethroid exposure and alterations in antioxidant status in rat erythrocytes: a possible involvement of reactive oxygen species. Toxicol. Lett. 105 (3), 197–205. https://doi.org/10.1016/S0378-4274(98)00399-3.

Kaur, G., Mehta, S.K., 2017. Developments of polysorbate (tween) based microemulsions: preclinical drug delivery, toxicity and antimicrobial applications. Int. J. Pharm. 529 (1–2), 134–160. https://doi.org/10.1016/j.ijpharm.2017.06.059.

Khuwaja, G., Khan, M.M., Ishrat, T., Ahmad, A., Raza, S.S., Ashafaq, M., Javed, H., Khan, M.B., Khan, A., Vaibhav, K., Safhi, M.M., Islam, F., 2011. Neuroprotective effects of curcumin on 6-hydroxydopamine-induced Parkinsonism in rats:

behavioral, neurochemical and immunohistochemical studies. Brain Res. 1368, 254–263. https://doi.org/10.1016/j.brainres.2010.10.023.

Liu, L., Gao, Q., Lu, X., Zhou, H., 2016. In situ forming hydrogels based on chitosan for drug delivery and tissue regeneration. Asian J. Pharm. Sci. 11 (6), 673–683. https://doi.org/10.1016/j.ajps.2016.07.001.

Longa, E.Z., Weinstein, P.R., Carlson, S., Cummins, R., 1989. Reversible middle cerebral artery occlusion without craniectomy in rats. Stroke 20, 84–91. https://doi.org/10.1161/01.STR.20.1.84.

Madsen, H.L., Andersen, C.M., Jørgensen, L.V., Skibsted, L.H., 2000. Radical scavenging by dietary flavonoids. A kinetic study of antioxidant efficiencies. Eur Food Res. Technol. 211 (4), 240–246. https://doi.org/10.1007/s002170000189.

Magiera, S., Baranowska, I., Kusa, J., 2012. Development and validation of UHPLC-ESI-MS/MS method for the determination of selected cardiovascular drugs, polyphenols and their metabolites in human urine. Talanta 89, 47–56. https://doi.org/10.1016/j.talanta.2011.11.055.

Mendonça, D.V., Lage, L.M., Lage, D.P., Chávez-Fumagalli, M.A., Ludolf, F., Roatt, B.M., Menezes-Souza, D., Faraco, A.A., Castilho, R.O., Tavares, C.A., Barichello, J.M., Duarte, M.C., Coelho, E.A., 2016. Poloxamer 407 (Pluronic(®) F127)-based polymeric micelles for amphotericin B: In vitro biological activity, toxicity and in vivo therapeutic efficacy against murine tegumentary leishmaniasis. Exp. Parasitol. 169, 34–42. https://doi.org/10.1016/j.exppara.2016.07.005.

Mohandas, J., Marshall, J.J., Duggin, G.G., Horvath, J.S., Tille, D.J., 1984. Differential distribution of glutathione and glutathione-related enzymes in rabbit kidney. Possible implications in analgesic nephropathy. Biochem. Pharmacol. 33 (1), 1801–1807. https://doi.org/10.1016/0006-2952(84)90353-8.

Napper, D., Netschey, A., 1971. Studies of the steric stabilization of colloidal particles. J. Colloid Interface Sci. 37 (3), 528–535. https://doi.org/10.1016/0021-9797(71)90330-4.

Ohkawa, H., Ohishi, N., Yagi, K., 1979. Assay for lipid peroxides in animal tissues by thiobarbituric acid reaction. Anal Biochem. 95 (2), 351–358. https://doi.org/10.1016/0003-2697(79)90738-3.

Otberg, N., Richter, H., Knuttel, A., Schaefer, H., Sterry, W., Lademann, J., 2004. Laser spectroscopic methods for the characterization of open and closed follicles. Laser Phys. Lett. 1 (1), 46–49. https://doi.org/10.1002/lapl.200310011.

Raeisi, S., Chavoshi, H., Mohammadi, M., Ghorbani, M., Sabzichi, M., Ramezani, F., 2019. Naringenin-loaded nano-structured lipid carrier fortifies oxaliplatindependent apoptosis in HT-29 cell line. Process Biochem. 83, 168–175. https://doi.org/10.1016/j.procbio.2019.05.013.

Raso, G.M., Meli, R., Di Carlo, G., Pacilio, M., Di Carlo, R., 2001. Inhibition of inducible nitric oxide synthase and cyclooxygenase-2 expression by flavonoids in macrophage J774A.1. Life Sci. 68 (8), 921–931. https://doi.org/10.1016/S0024-3205(00)00999-1.

Raza, S.S., Khan, M.M., Ahmad, A., Ashafaq, M., Islam, F., Wagner, A.P., Safhi, M.M., Islam, F., 2013. Neuroprotective effect of naringenin is mediated through suppression of NF-κB signaling pathway in experimental stroke. Neuroscience 230, 157–171. https://doi.org/10.1016/j.neuroscience.2012.10.041.

Renugadevi, J., Prabu, S.M., 2009. Naringenin protects against cadmium-induced oxidative renal dysfunction in rats. Toxicology 256, 128–134. https://doi.org/10.1016/j.tox.2008.11.012.

Rey-Rico, A., Venkatesan, J.K., Frisch, J., Rial-Hermida, I., Schmitt, G., Concheiro, A., Madry, H., Alvarez-Lorenzo, C., Cucchiarini, M., 2015. PEO-PPO-PEO micelles as effective rAAV-mediated gene delivery systems to target human mesenchymal stem cells without altering their differentiation potency. Acta Biomater. 27, 42–52. https://doi.org/10.1016/j.actbio.2015.08.046.

Salatin, S., Barar, J., Barzegar-Jalali, M., Adibkia, K., Jelvehgari, M., 2017. Thermosensitive in situ nanocomposite of rivastigmine hydrogen tartrate as an intranasal delivery system: Development, characterization, ex vivo permeation and cellular studies. Colloids Surf. B Biointerfaces. 159, 629–638. https://doi.org/10.1016/j.colsurfb.2017.08.031.

Siepmann, J., Peppas, N.A., 2001. Modeling of drug release from delivery systems based on hydroxypropyl methylcellulose (HPMC). Adv. Drug Deliv. Rev. 48 (2–3), 139–157. https://doi.org/10.1016/S0169-409X(01)00112-0.

Singh, R.M., Kumar, A., Pathak, K., 2013. Thermally triggered mucoadhesive in situ gel of loratadine: β-cyclodextrin complex for nasal delivery. AAPS PharmSciTech. 14 (1), 412–424. https://doi.org/10.1208/s12249-013-9921-9.

Sumathi, R., Tamizharasi, S., Sivakumar, T., 2017. Formulation and evaluation of polymeric nanosuspension of naringenin. Int. J. App. Pharm. 9 (6), 60–70. https://doi.org/10.22159/ijap.2017v9i6.21674.

Sun, M., Zhao, Y., Gu, Y., Xu, C., 2009. Inhibition of nNOS reduces ischemic cell death through down-regulating calpain and caspase-3 after experimental stroke. Neurochem. Int. 54 (5–6), 339–346. https://doi.org/10.1016/j.neuint.2008.12.017.

Sun, Z., Zhao, L., Zuo, L., Qi, C., Zhao, P., Hou, X., 2014. A UHPLC-MS/MS method for simultaneous determination of six flavonoids, gallic acid and 5,8-dihydroxy-1,4-naphthoquinone in rat plasma and its application to a pharmacokinetic study of Cortex Juglandis Mandshuricae extract. J. Chromatogr. B Analyt. Technol. Biomed. Life Sci. 958, 55–62. https://doi.org/10.1016/j.jchromb.2014.03.013.

Ur-Rehman, T., Tavelin, S., Gröbner, G., 2011. Chitosan in situ gelation for improved drug loading and retention in poloxamer 407 gels. Int. J. Pharm. 409 (1–2), 19–29. https://doi.org/10.1016/j.ijpharm.2011.02.017.

Wang, X., Chen, Z., Huang, J., Huang, L., Luo, N., Liang, X., Liang, M., Xie, W., 2017a. Naringenin prevents ischaemic stroke damage via anti-apoptotic and anti-oxidant effects. Clin. Exp. Pharmacol. Physiol. 44 (8), 862–871. https://doi.org/10.1111/1440-1681.12775.

Wang, X., Zhao, X., Gu, L., Lv, C., He, B., Liu, Z., Hou, P., Bi, K., Chen, X., 2014. Simultaneous determination of five free and total flavonoids in rat plasma by ultra HPLC-MS/MS and its application to a comparative pharmacokinetic study in normal and hyperlipidemic rats. J. Chromatogr. B Analyt. Technol. Biomed. Life Sci. 953–954, 1–10. https://doi.org/10.1016/j.jchromb.2014.01.042.

Wang, Y., Jiang, S., Wang, H., Bie, H., 2017b. A mucoadhesive, thermoreversible in situ nasal gel of geniposide for neurodegenerative diseases. PLoS ONE 12, (12). https://doi.org/10.1371/journal.pone.0189478 e0189478.

Xu, X., Shen, Y., Wang, W., Sun, C., Li, C., Xiong, Y., Tu, J., 2014. Preparation and in vitro characterization of thermosensitive and mucoadhesive hydrogels for nasal delivery of phenylephrine hydrochloride. Eur. J. Pharm. Biopharm. 88 (3), 998–1004. https://doi.org/10.1016/j.ejpb.2014.08.015.

Yu, J., Wang, L., Walzem, R., Miller, E.G., Pike, L.M., Patil, B.S., 2005. Antioxidant activity of citrus limonoids, flavonoids, and coumarins. J. Agric. Food Chem. 53 (6), 2009–2014. https://doi.org/10.1021/jf0484632.

Zafar, K.S., Siddiqui, A., Sayeed, I., Ahmad, M., Salim, S., Islam, F., 2003. Dose-dependent protective effect of selenium in rat model of Parkinson's disease: neurobehavioral and neurochemical evidences. J. Neurochem. 84 (3), 438–446. https://doi.org/10.1046/j.1471-4159.2003.01531.x.

Zhang, L., Parsons, D.L., Navarre, C., Kompella, U.B., 2002. Development and in-vitro evaluation of sustained release poloxamer 407 (P407) gel formulations of ceftiofur. J. Control Release. 85 (1–3), 73–81. https://doi.org/10.1016/S0168-3659(02)00273-0.

Zhao, Y.Z., Jin, R.R., Yang, W., Xiang, Q., Yu, W.Z., Lin, Q., Tian, F.R., Mao, K.L., Lv, C.Z., Wáng, Y.X., Lu, C.T., 2016. Using gelatin nanoparticle mediated intranasal delivery of neuropeptide substance P to enhance neuro-recovery in hemiparkinsonian rats. PLoS ONE 11, (2). https://doi.org/10.1371/journal.pone.0148848 e0148848.

Further reading

Ahmed, S., Gull, A., Aqil, M., Ansari, M.D., Sultana, Y., 2019. Poloxamer-407 thickened lipid colloidal system of agomelatine for brain targeting: characterization, brain pharmacokinetic study and behavioral study on Wistar rats. Colloids Surf. B Biointerf. 181, 426–436. https://doi.org/10.1016/j.colsurfb.2019.05.016.

US FDA. Guidance for Industry Bioanalytical Method Validation; 2001. Available from: http://www.fda.gov/downloads/Drugs/GuidanceComplianceRegulatoryInformation/Guidances/UCM070107.pdf. [Last accessed on 2018 May 24].